# Numerical Calculation and Data Visualization Tool for Cosmological Physics: QuintET

by

Ephraim Adane Tekle

B.S. in Physics, Massachusetts Institute of Technology (2001)
B.S. in Mathematics, Massachusetts Institute of Technology (2001)

Submitted to the Department of Civil and Environmental Engineering in partial fulfillment of the requirements for the degree of

Master of Engineering in Civil and Environmental Engineering

at the

MASSACHUSETTS INSTITUTE OF TECHNOLOGY

June 2003





Author .....
Department of Civil and Environmental Engineering
May 9, 2003

Certified by .....
George A Kocur
Senior Lecturer
Thesis Supervisor

Accepted by .....
Oral Buyukozturk
Chairman, Department Committee of Graduate Students

# Numerical Calculation and Data Visualization Tool for Cosmological Physics: QuintET

by

Ephraim Adane Tekle

Submitted to the Department of Civil and Environmental Engineering
on May 9, 2003, in partial fulfillment of the
requirements for the degree of
Master of Engineering in Civil and Environmental Engineering

## Abstract

In Cosmological Physics today, theoretical study and numerical simulations dominate over observation. With the vast arrays of physical and technological barriers to make cosmologically significant observations, theories and hypotheses are tested primarily on their confirmability with the small and limited astrophysical data available. The lack of data pertaining to the cosmological scale and the heavily coupled partial differential equations normally associated with cosmological physics require numerical simulation and superb data visualization tools. Furthermore, since it is implausible to do any kind of experimentation in a laboratory setting to distinguish between cosmological theories, numerical simulation remains to be the only viable solution to take on that task by deducing from the 'digital' universes, which model best fits all available cosmological data. Recent space based observatories, such as the Microwave Anisotropy Probe (MAP), and ambitious new ways of looking at the universe through gravitational–wave detection will expose many features of the universe and narrow down the long list of plausible cosmological models. This thesis briefly discusses various numerical simulations and data visualization tools, and presents a detailed case study of a numerical simulation and data visualization tool, dubbed QuintET, developed for the study of quintessence cosmological models.

Thesis Supervisor: George A Kocur
Title: Senior Lecturer

# Acknowledgments

I would like to thank Dr. Kocur for his guidance on this project and during the last nine months in the Information Technology program with the Civil and Environmental Engineering department. I would also like to thank Professor Alan Guth for the years of guidance and support throughout my MIT academic career and for the privilege to have worked with him. I would also like to thank the physics department for generously funding my graduate studies over the last two years. I would like to thank the professors, friends and classmates I had the privilege of meeting during the last five years, thank you for making my MIT experience the most memorable and educational one. Last but not least, I would like to thank my wife Sophia for her undying support and understanding.

# Contents


**1 Introduction** **13**

**2 Quintessence** **15**

2.1 Background . . . . . 15

2.2 Governing Equations . . . . . 18

2.3 Parameters and Initial Conditions . . . . . 20

2.4 Algorithm . . . . . 21

**3 QuintET** **25**

3.1 Design . . . . . 27

3.1.1 Design Structure . . . . . 27

3.1.2 Data Format: Inheritance . . . . . 27

3.1.3 Extensibility . . . . . 28

3.2 Usage . . . . . 30

3.2.1 Settings . . . . . 30

3.2.2 Data . . . . . 32

3.2.3 Plot . . . . . 34

3.2.4 Miscellaneous . . . . . 40

3.3 Future Work . . . . . 45

**4 Conclusion** **47**

**A Scalar Field–Curvature Coupling** **49**

**B Equation of Motion of the Scale Factor $R$** **57**

**C Equation of Motion for $\phi$** **61**

**D Java 2 SDK Packages** **63**

# List of Figures


3-1 QuintET class diagram. . . . . 26
3-2 Calculation settings, selection, control and log. . . . . 29
3-3 Initial and 'boundary' conditions. . . . . 30
3-4 Calculation selection. . . . . 31
3-5 Time evolution calculations. . . . . 31
3-6 $w_Q$–$\Omega_m$ calculation. . . . . 32
3-7 Data view. . . . . 33
3-8 The `Setting` menu. . . . . 34
3-9 Data visualization. . . . . 35
3-10 The pop–up visualization toolkit. . . . . 36
3-11 The zooming interface. . . . . 38
3-12 The text and label interface. . . . . 39
3-13 Axes properties and data source. . . . . 40
3-14 Saving plot. . . . . 41
3-15 The main menu. . . . . 42
3-16 The `File` menu. . . . . 42
3-17 The `View` menu. . . . . 43
3-18 The `Help` menu. . . . . 44
3-19 Error log. . . . . 44

# List of Tables

D.1 QuintET primary Java 2 SDK packages. . . . . 64

# Chapter 1

# Introduction

For a very long time and even today physicist at leading institutes and national labs use procedural programming languages, such as FORTRAN, to carry out their numerical calculations and data analysis. Although still very popular, these environments do not scale up to the challenges of today's particle accelerators and numerical calculation needs. Today, there are over a dozen of experiments that produce over a Terabytes of raw data per run, and the complexity of the data analysis scheme required for such a large volume of data demands a transition to modern software development tools and practices.

The progress made in Computer Science over the last two decade, particularly in the area of Object-Oriented design and development, allowed for the development of large–scale data analysis tools such as ROOT [4], Matlab [9], etc. Furthermore, Object-Oriented programming allowed for the development of complex data analysis and numerical calculation tools with a relatively short development time.

QuintET, the numerical calculations and data visualization tool I developed and discuss in this thesis, is designed for the study of cosmological models. Before going straight to discussing the software, I will first present the necessary background needed to understand what the system does. The appendices present a step by step derivation of the main equations behind quintessence.

# Chapter 2

# Quintessence

## 2.1 Background

[1]Until about the early 1900s, most scientist thought that we live in a static universe. When Albert Einstein first applied his General Theory of Relativity in 1917 to the universe as a whole, he realized that a static solution to his equation did not exist. According to the general theory of relativity, the gravitational force between material objects is always attractive. Einstein realized that by adding a repulsive term, which he called the cosmological constant ($\Lambda$), his equation allows for a static universe solution.

After Edwin Hubble's convincing demonstration in the 1920s that the universe is expanding, Einstein quickly discarded his cosmological constant, calling it his greatest blunder. Hubble's observation strongly suggest that distant galaxies are receding from us with a velocity that is proportional to their distance. Thus one can write

$$\mathbf{v} = H\mathbf{r},$$

where $\mathbf{v}$ is the recession velocity, $\mathbf{r}$ is the distance to the galaxy and $H$ is the Hubble constant.

[1]Some of the work presented here is taken from my research in cosmological physics with Professor Alan Guth, Department of Physics, Massachusetts Institute of Technology.

If the universe is expanding according to the Hubble's Law, then one can extrapolate the expansion backwards in time to an instant when all the galaxies must have been at the same point and the universe would have an infinite density. Current estimates put that instant, dubbed the *Big Bang*, about 10 to 20 billion years ago.

In addition to Hubble's law, much observational evidence was found in support of the big bang theory. Two important pieces of evidence are the Cosmic Background Radiation (CMB) and the big bang nucleosynthesis. Despite of its success in explaining the evolution of the universe since about one second after the big bang, the standard big bang model leaves very obvious questions unanswered. The initial conditions of the big bang look peculiar and are assumed without any explanation. The following list encapsulates the main problems with this theory.

**The Horizon Problem** How did the universe become so homogeneous on large scales? The horizon at last scattering ($Z \sim 1000$) subtends an angle about one degree. How did then universe, which largely consists of causally disconnected regions, became homogeneous on large scale?

**The Flatness Problem** Why was the mass density of the early universe so extraordinarily close to the critical density–equal up to the fifteenth decimal place?

**The Structure Problem** The universe is not precisely homogeneous. This model does not give an explanation for the origin or the form of these inhomogeneities.

**The Expansion Problem** What caused the initial expansion of the early universe?

In rescue of the big bang theory came a new theory, which is a blend of particle physics—the physics of elementary particles, governed by quantum theory—and cosmology—the physics of space–time and energy, governed by relativity theory. The mechanism of this new theory, the Inflationary Theory, which was first proposed by Alan Guth in 1981, depends on scalar fields.

As technology progresses, new and improved methods of probing the far reaches of the universe becomes possible. Early supernovae study suggest that supernovae could be used as standard candles for cosmological measurements [7]. In the late

1980s, with the discovery of a more homogeneous subclass of type Ia supernovae [7], determination of cosmological parameters became feasible. The Supernova Cosmology Project, started in 1988 [7], specially made it possible to measure supernovae events with a high–redshift enough to determine cosmological parameters of the universe such as the deceleration parameter. Analysis of recent observations by [7] and other groups suggest that the expansion of the universe might be accelerating. Furthermore, preliminary analysis of data from MAP suggest that the equation–of–state of the universe is negative (i.e. the universe is permeated with an exotic form of matter that produces a long–range repulsive gravitational force). If these observations are true, and most scientist agree they are, then a good fraction of the energy content of the universe must have negative pressure. Currently, there are two explanations. One is a none–zero cosmological constant, and the other is that the universe is being accelerate by the gravitational repulsion caused by Quintessence—a slowly evolving scalar field that permeates the universe.

Quintessence not only beautifully solves the accelerating expansion problem, but also addresses the coincidence problem that the none–zero cosmological constant scenario does not address.

As the universe expands, the energy density associated with the different constituent elements (photon, neutrino, baryonic matter, cosmological constant and/or quintessence, etc.) evolve in different rates. This fact in conjunction with observations, require that the ratio of the energy density of the element that is responsible for the accelerated expansion to that of everything else must be set to a specific, infinitesimal value in the early universe. This problem is avoided under a subclass of quintessence that allow for tracking solutions.

The mathematics of this model of quintessence, dubbed "tracker field," is explored in appendices (A), (B) and (C). In the following few sections, I will quote the equations required in QuintET and modify them to allow for numerical calculations.

## 2.2 Governing Equations

From appendices (B) and (C), only equations ( B.25), ( B.26) and ( C.9) are required to carry out quintessence calculations. In order to carry out numerical calculations, however, we need to modify these equations so that unitless variables are obtained. After setting $\xi \approx 0$, these equations give:

$$H^2 \equiv \left(\frac{\dot{R}}{R}\right)^2 = \frac{8\pi}{3}G(\rho_T), \tag{2.1}$$

$$\frac{\ddot{R}}{R} = -\frac{4\pi}{3}G(\rho_T + 3p_T), \tag{2.2}$$

$$\ddot{Q} + 3H\dot{Q} + dV/dQ = 0, \tag{2.3}$$

where $Q$ has been substituted in place of $\phi$, and $\rho_T$ and $p_T$ are the total energy density and pressure densities of the universe as given by $T_{00}$ (equation ( B.19)) and $T_{11}$ (equation ( B.24)) terms, respectively. It is believed that the energy content of the universe is primarily composed of quintessence, cold–dark matter (or ordinary matter), radiation, and neutrino. Furthermore, the energy density of ordinary matter scales as $\rho_m \propto R^{-3}$, and that of radiation scales as $\rho_\gamma \propto R^{-4}$. Assuming neutrinos are massless, the neutrino energy density $\rho_\nu$ also scales as that of radiation. Therefore, the time dependency of these energy densities could be written as:

$$\rho_i = \left[\frac{R(t_o)}{R(t)}\right]^j \rho_{i,o} \tag{2.4}$$

where $i$ is anyone of $m, \gamma$, or $\nu$; and $j$ is the appropriate power dependency. Subscript "$_o$" refers to any reference time[2]. With the following definitions

$$\rho_c \equiv \frac{3H^2}{8\pi G}, \quad \text{and} \quad \Omega_i \equiv \frac{\rho_i}{\rho_c}, \tag{2.5}$$

[2]The reference time is chosen based on available observational data or theoretical prediction that determine one or more cosmological variables, such as the energy densities, with some level of confidence. It is also when the redshift, $Z$, is zero in this model. In this thesis, the reference time is assumed to be the current era where $\Omega_m \approx 0.3$. The numerical simulation package developed allows for this value to vary.

equation (2.4) can to rewritten as

$$\rho_i = \rho_{c,o}\Omega_{i,o}\left[\frac{R(t_o)}{R(t)}\right]^j. \tag{2.6}$$

We now define the main unit–less quantity $x$ in this calculation as

$$x \equiv \frac{R(t)}{R(t_o)}. \tag{2.7}$$

Therefore equation (2.1) can be rewritten as

$$\left(\frac{\dot{x}}{x}\right)^2 = H_o^2\left\{\Omega_{\gamma,o}x^{-4} + \Omega_{\nu,o}x^{-4} + \Omega_{m,o}x^{-3} + \bar{\Omega}_Q(t)\right\},$$

where $\bar{\Omega}_Q = \rho_Q/\rho_{c,o}$. The above equation could also be rewritten as follow in order to make the first derivative of $x$ more transparent:

$$\dot{x} = \frac{H_o}{x}\left[\bar{\Omega}_Q(t)\,x^4 + \Omega_{m,o}x + \Omega_{\gamma+\nu,o}\right]^{\frac{1}{2}}. \tag{2.8}$$

Furthermore, if the above equation is evaluated at $t = t_o$, we obtain $\Omega_{Q+m+\gamma+\nu} = 1$, as required for a flat universe[3]. QuintET employs Taylor expansions to carry out the numerical calculation; hence, by taking the derivative of equation (2.8), we obtain an expression for the second derivative of $x$:

$$\ddot{x} = \frac{1}{2\dot{x}}\left\{\left[\left(\frac{H_o}{x}\right)^2\left(4\bar{\Omega}_Q x^3 + \Omega_{m,o}\right) - 2H\dot{x}\right]\dot{x} + (H_o x)^2\frac{\dot{Q}}{\rho_{c,o}}\left[\frac{dV}{dQ} + \ddot{Q}\right]\right\}. \tag{2.9}$$

With this results, we are now set to carry out the calculation. Since the equations described above are two non–linear second–order coupled differential equations, we need to set a few initial conditions on $x$ ($x$ and $\dot{x}$ for instances) and and on $Q$ (similarly $Q$ and $\dot{Q}$). Furthermore, some quantities, such as the current value of Hubble's *constant*, the current background energy densities, the current critical energy density of the universe must be set. Finally, $V[Q]$ also must be fixed to have a specific form.

[3]In accordance with the inflationary theory and observation, in all calculations the background space–time is assumed to be given by the flat ($k = 0$) Robertson-Walker metric.

## 2.3 Parameters and Initial Conditions

QuintET is equipped to handle the following form for the potential energy:

$$V_\alpha[Q] = M^4 \left(\frac{M_p}{Q}\right)^\alpha, \tag{2.10}$$

where $M$ is the only free parameter and $M_p = 1.22 \times 10^{19}\ GeV$ is the Plank mass and $\alpha$ is an integer greater than one. These potentials allow for a tracker solution [15]. Furthermore, we can also construct an exponential potential from these by summing all powers of $\alpha$, as follows:

$$V[Q] = \sum_{\alpha=1}^{\infty} \frac{V_\alpha}{\alpha!} = M^4 \left[\exp^{\left(\frac{M_p}{Q}\right)} - 1\right]. \tag{2.11}$$

The single most important parameter in cosmology is perhaps the Hubble's *constant*, which measures how fast galaxies are receding away from us. Its value today is estimated to be

$$H_{today} \equiv H_o h \times (9.78 \times 10^9 yr)^{-1},$$

where $h$ is the Hubble parameter and estimated to lie between 0.4 and 1 [8]. Using equation (2.5) and the above result, one obtains

$$\rho_{c,0} \equiv \rho_c(t_0) = 8.03 \times 10^{-47} h^2\ GeV^4.$$

With the critical energy at $t = t_o$ determined, solving for either the omegas or the energy densities is exactly the same. Therefore we use $\Omega_{Q+m+\gamma+\nu} = 1$ to eliminate one parameter and obtain the values for remaining three energy densities.

Black–body electromagnetic radiation has an energy density given by

$$\rho(t) = \frac{\pi^2[KT(t)]^4}{15(\hbar c)^3}, \tag{2.12}$$

where $K$ is the Boltzmann's constant. Since we know from the thermal cosmic background radiation that the universe 'glows' at a temperature $2.735K$ [6], we can use

equation (2.12) to calculate the photon energy density, and subsequently $\Omega_{\gamma,o}$. Putting this value for temperature in equation (2.12) and using (2.5) we obtain

$$\Omega_{\gamma,o} = 1.0 \times 10^{-4}.$$

Furthermore, the decoupling of neutrinos preceded the decoupling of photons in the early universe. Using the decoupling temperature of neutrinos and photons, one can infer the ratio of their temperature must satisfy

$$T_\nu = \left(\frac{4}{11}\right)^{1/3} T_\gamma.$$

Using the observed photon temperature today, we can deduce the existence of a neutrino background with temperature $T_\nu = 1.95K$. Using equations (2.5) and (2.12) we get

$$\Omega\nu, o = 2.6 \times 10^{-5}.$$

One free parameter whose value must be determined is $M$. If $\Omega_{m,o} \approx 0.3$, as astronomical observation suggest, $\Omega_{Q,o} = \Omega_{T-(m+\gamma+\nu)} \approx 0.7$. Here is where we must fine–tune the only free parameter $M$ in our equations in order to obtain the desired $\Omega_{Q,o}$ value ($\approx 0.7$). In the numerical calculations, this was done by first estimating the value of $Q$ and $\dot{Q}$, hence $\rho_{Q,o}$, at some reference time then recursively adjusting $M$ until the desired result is obtained. To get an order–of–magnitude estimation, we can proceed as follows. In order to get $\Omega_{Q,o} \approx 0.7$ requires $V(Q \approx M_p) \approx \rho_{m,o} = \Omega m, o \times \rho_{c,0}$ [15]. This imposes the constraint

$$M^4 \approx \left(\frac{\Omega m, o \times \rho_{c,o}}{e-1}\right) \approx 10^{-48}\ (GeV)^4.$$

## 2.4 Algorithm

In order to employ numerical methods, as discussed above, it is necessary that we fix the initial conditions. One can see that there are only three independent variables in

these equations; hence setting $x(t_i)$, $Q(t_i)$ and $\dot{Q}(t_i)$, where $i$ stands for initial and not the reference time, suffices to numerically solve the coupled differential equations and obtain numerical estimates of all the relevant quantities. The initial values of $Q$ and $\rho_Q$ are only limited by the range of initial conditions the quintessence model permits. A weak constraint consists of $\rho_{Q,i}$ must be large enough but smaller than the background energy density so that $Q$ begins tracking today. The following is an example of initial conditions used:

- $x(t_i) = 1 \times 10^{-14}$,
- $Q(t_i) = 2.17 \times 10^{17}\ GeV$, and
- $\dot{Q}(t_i) = 1 \times 10^{-30}\ (GeV)^2$.

As you will see in the next chapter, it is possible to manually and systematically change these values in QuintET.

The numerical calculation was carried out by calculating the first few orders of $x$, $\dot{Q}$ and $Q$ in Taylor expansion with higher order correction terms. Since the rate of change of $x$ varies greatly for the $1/x > 1$ and $1/x < 1$ eras, the time division $dt$ also varied as well. In QuintET, this was set as $dt = 10^{\log x \log \dot{x} - 3}$. Therefore, a thousand calculations were done for each order of $x$. In turn, $x$ varied from about $10^{-20}$ to $10^{380}$, which roughly results in $300,000$ times number of variables calculated data points per run. This is an enormous memory load.

Taking $x$ as an example, the following steps illustrate how the numerical integration was carried out:

1. $\dot{x}(i)$ (from equation (2.8))
2. $\ddot{x}(i)$ (from equation (2.9))
3. $x(i+1) = x(i) + \dot{x}(i)dt + \frac{1}{2}\ddot{x}(i)dt^2$ (first approximation)
4. $\dot{x}(i+1)$ (from equation (2.8))
5. $\ddot{x}(i+1)$ (from equation (2.9))

6. $x(i+1) = x(i) + \dot{x}(i)dt + \frac{1}{2}\ddot{x}(i)dt^2 + \frac{1}{3!}\left(\frac{\ddot{x}(i+1)-\ddot{x}(i)}{dt}\right)dt^3$ (final approximation)

Since $1/(Z+1)$ *equivx* $\geq 0$, therefore $Z+1 \geq 0$, numerical calculations were terminated when[4] $Z = -1$.

[4]Due to the nature of floating–point calculations, the calculation in fact stopped when $Z + 1 \approx 10^{-308}$.

# Chapter 3

# QuintET

QuintET features tools to numerically calculate cosmological parameters as well as an elaborately designed data visualization tool to help analyze cosmological data. QuintET is developed using the Java 2 SDK 1.4. The primary packages used along with their descriptions are given in table (D.1). The following few sections will briefly discuss the different aspects and features of QuintET.

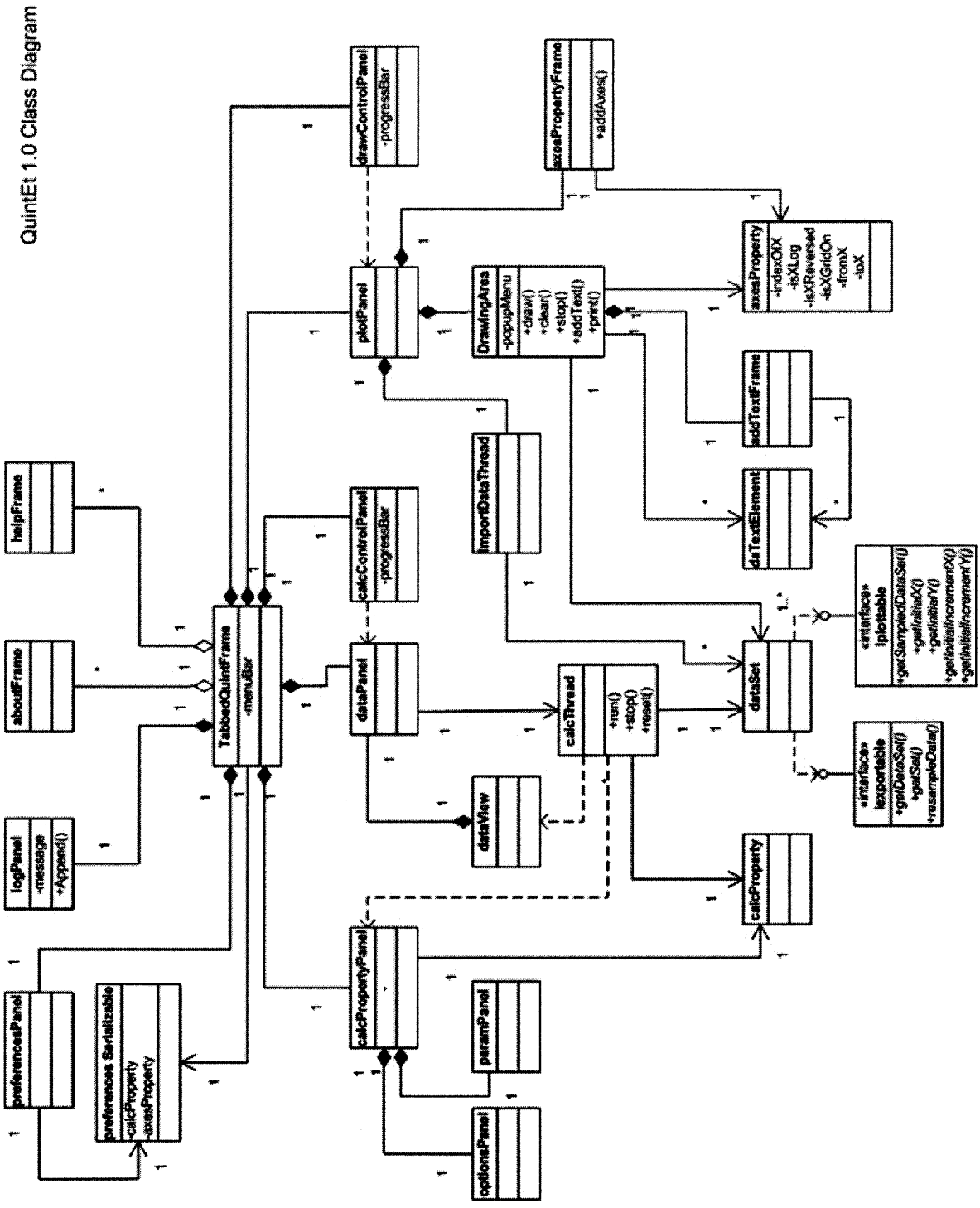


Figure 3-1: QuintET class diagram

## 3.1 Design

### 3.1.1 Design Structure

QuintET is design with modularity in mind[1]. The `TabbedQuintFrame` class acts like a hub where each of the different engines (calculation, plot, etc.) and components (help, menu, etc.) plug–in. Overall, the application has 23 primary classes and 2 interfaces. The total number of classes including inner classes exceeds 100. The application has a centralized `serializable` preferences class where calculation and plot settings (discussed below) as well as general user preferences (such as option to zip saved files) are stored. The following is a brief discussion of the two main classes that handle numerical calculation and data plotting behind the scene.

`calculationThread` This class, which runs on a separate `Thread`, is used by the calculation engine which is part of the calculation component. This particular component, along with its classes (`calculationThread` is one of them) is designed specifically for quintessence calculations. Other components that do other calculations can be added as discussed below. The data generated is stored in a class that extends the `Iplottable` and the `Iexportable` interfaces so as to allow for the plotting and saving, respectively, of the data.

`drawingArea` The `drawingArea` class, which also runs on a separate `Thread`, is part of the plotting component. This component, along with all of its classes, is designed to handle any data that implements the `Iplottable` interface (discussed below) irrespective of its source.

### 3.1.2 Data Format: Inheritance

One features of QuintET's modular design that deserves special treatment is the data format. The two interfaces in the application, namely `Iexportable` and `Iplottable`, determine if a data has the correct format to be displayed or/and to be plotted. The

[1]Please refer to figure (3-1) throughout this section

data set that is handled by the data displaying component and the data plotting component must implement the `Iexportable` and `Iplottable`, respectively. Amongst other features, each plottable data set must contain a method to sample its content given a density parameter.

### 3.1.3 Extensibility

The data plotting and displaying components make no distinction whether the data is obtained from a calculation or was imported from a file as long as the specified format is met. Therefore, these two components could be used in a number of ways. For instances, a component that carries out market analysis calculation can be implemented conveniently to use the data displaying and plotting (along with data and plot saving, etc.) capabilities of these two components.

Furthermore, as discussed above, these components plug–in to the hub in a fairly straightforward manner. Therefore, additional components can be designed and extend the system.

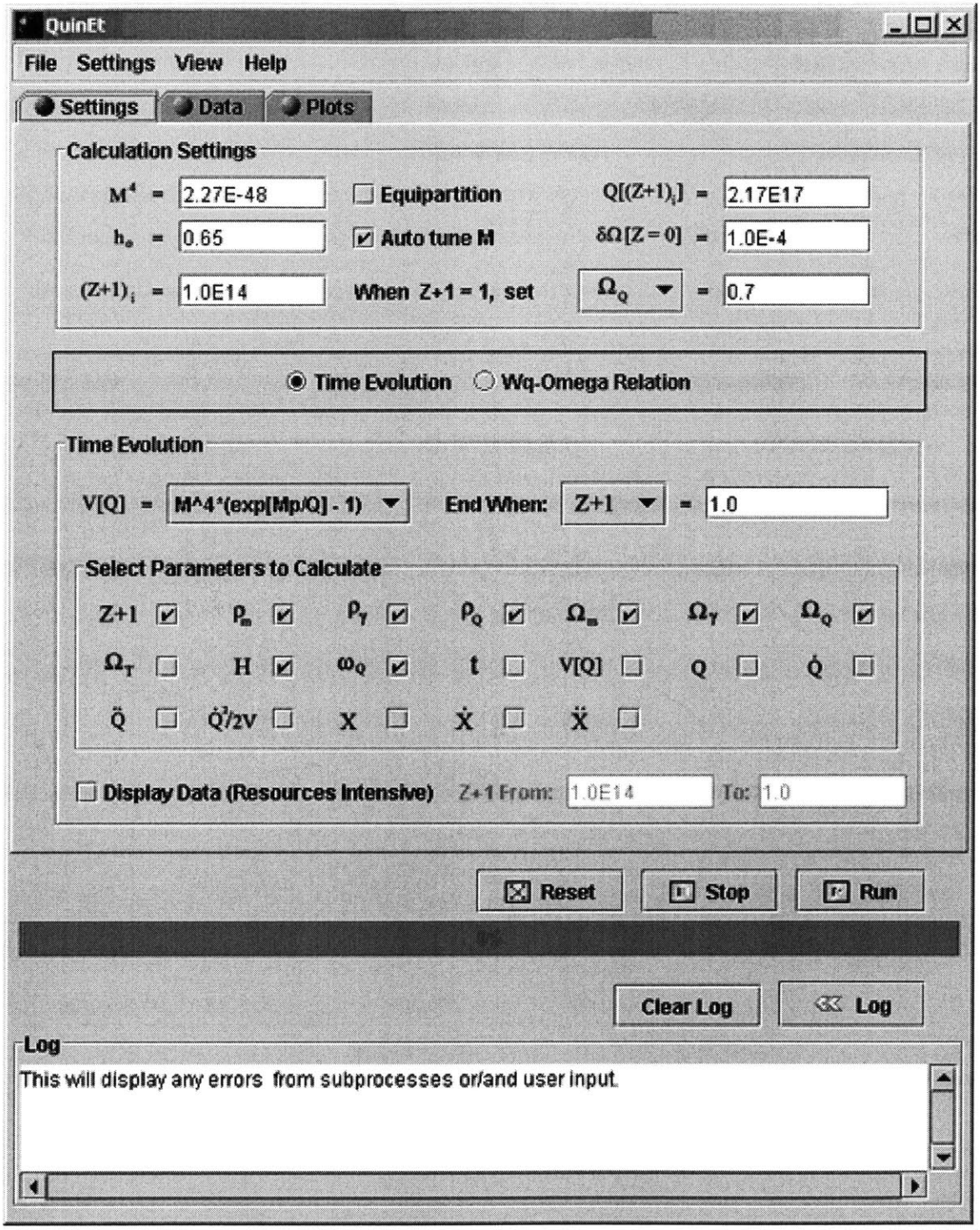


Figure 3-2: Calculation settings, selection and control, along with a retractable log panel.

## 3.2 Usage

Herein is presented a complete user documentation of QuintET. Figure (3-2) shows the calculation settings, selection and control tab, along with the Log panel. The following few sections will elaborate on the different features of the application.

### 3.2.1 Settings

All information pertaining to the initial and 'boundary' condition of the universe is specified here. $M^4$ is the only fine–tune parameter that needs to be carefully selected so as the $\Omega$ selected (refer to figure (3-3)) has the desired value. $h_o$ is the Hubble parameter and is estimated to lie between 0.4 and 1 [8]. $(Z+1)_i$ is set to $10^{-14}$ by default for convenience, but can be set as early as the end of inflation [8]. If `Equipartition`[2] is selected, then equipartition after inflation is assumed and $Q[(Z+1)_i]$, the initial quintessence field strength, is calculated based on that assumption. Otherwise, $Q[(Z+1)_i]$ must be specified. As discussed previously in this thesis, over 100 orders of magnitude variation in the initial condition of this field are accommodate for in the quintessence model.

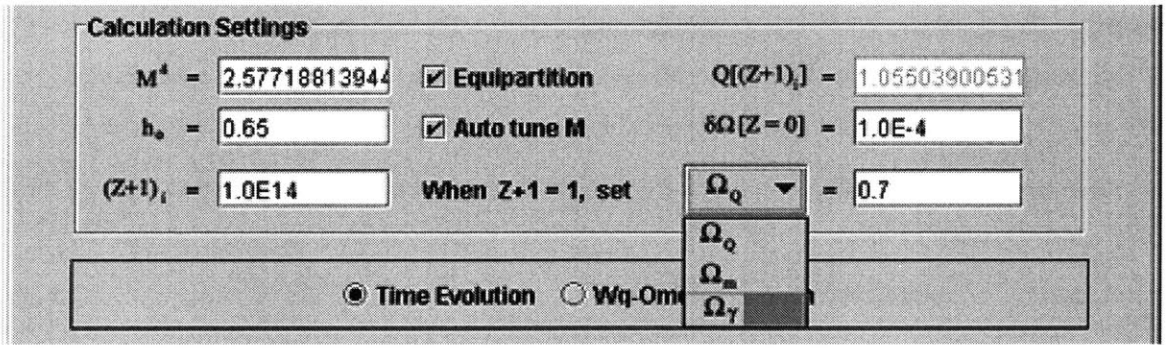


Figure 3-3: Initial and 'boundary' conditions. These parameters must be determined in order to carry out the numerical calculation

An alternative to setting $M^4$ manually, is to have the application determine the appropriate value by selecting the `Auto tune M`. In this case, the calculation runs until whichever initial $\Omega$ is selected, the application makes sure the absolute value of

[2]If this is selected, it is crucial that `Auto tune M` is also selected.

the difference between the specified value and the calculated value is less than what is specified in the $\delta\Omega[Z = 0]$ field.

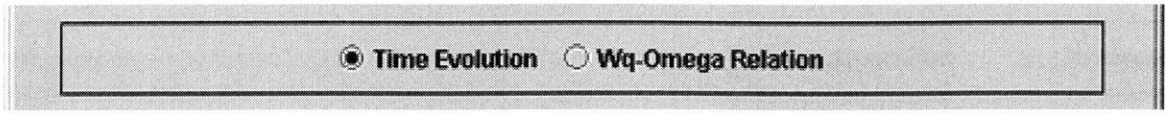


Figure 3-4: Determines which of the two calculations to carry out.

The calculation component that is deployed with this release of QuintET can carry out two types of calculation. While the first type, `Time Evolution`, carries out all calculation based on a specific model for the energy content of the universe, the second, `Wq--Omega Relation`, compares $W_q$ against $\Omega_m$ for different models, which can then be compared against astrophysical data.

### Time Evolution

In order to carry out `Time Evolution` calculations, the following three must be set: what model (or equally what potential), when should calculation end (in redshift), and which variables to calculate (see figure (3-5)). Seventeen parameters can be calculated in this mode, and the data can also be displayed directly. Displaying data, however, is very resources intensive and is disabled by default.

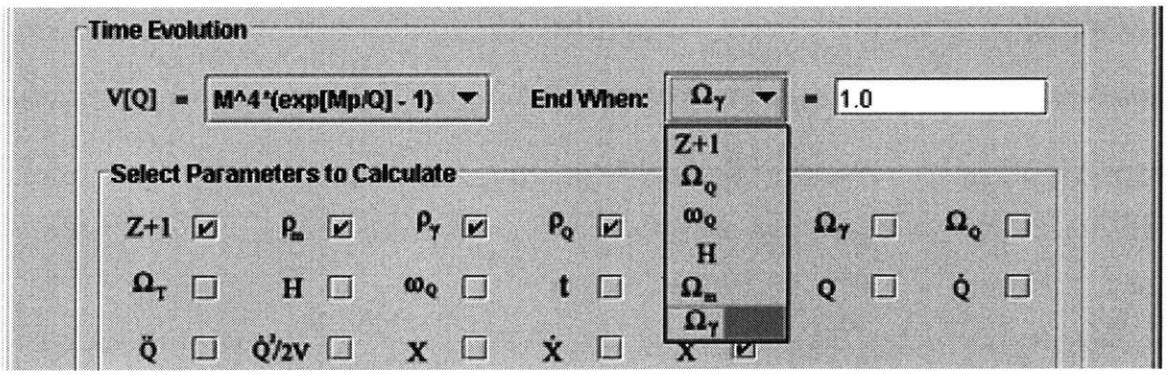


Figure 3-5: Time evolution calculations. From here, one can set the Quintessence potential and the end calculation parameter as well as which parameters to calculate and save in memory. Data can be displayed by selecting the appropriate check–box, however this consumes considerable amount of system resources.

$W_q$–$\Omega_m$

$W_q$–$\Omega_m$ calculations are done for different models over a range of $Omega_m$, and for this reason they take a considerable amount of time to complete. Either or both of the exponential potential and the inverse power law potential can be selected. For the inverse power law, the range of the power must also be set. The range of $\Omega_m$ to use must also be provided in order to carry out these calculations. Finally, the data can be displayed directly, although this feature is disabled by default.

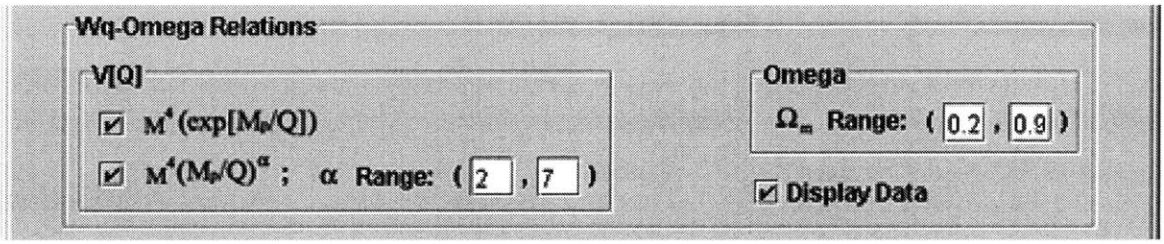


Figure 3-6: $w_q$–$\Omega_m$ calculations.

### 3.2.2 Data

The data generated by the calculation or imported from a file can be directly displayed in the `Data` component. Any data source that implements the `Iexportable` interface can be displayed here (refer to figure 3-7). The table itself is an extension of the `JTable` class (see table (D.1)), enhanced to allow for the requirements of QuintET.

#### Saving Data

Any column from the data view can be selected by clicking at any given cell, and multiple columns can be selected by pressing the the "Control" button while selecting cells of different columns. These selected columns can be saved into a file by either pressing the "Control" and "s" keys simultaneously or by selecting "Save data" from the "File" menu. Saving as well as importing of zipped files (see figure (3-8)) is supported and is recommended when saving/importing a very large set of data.

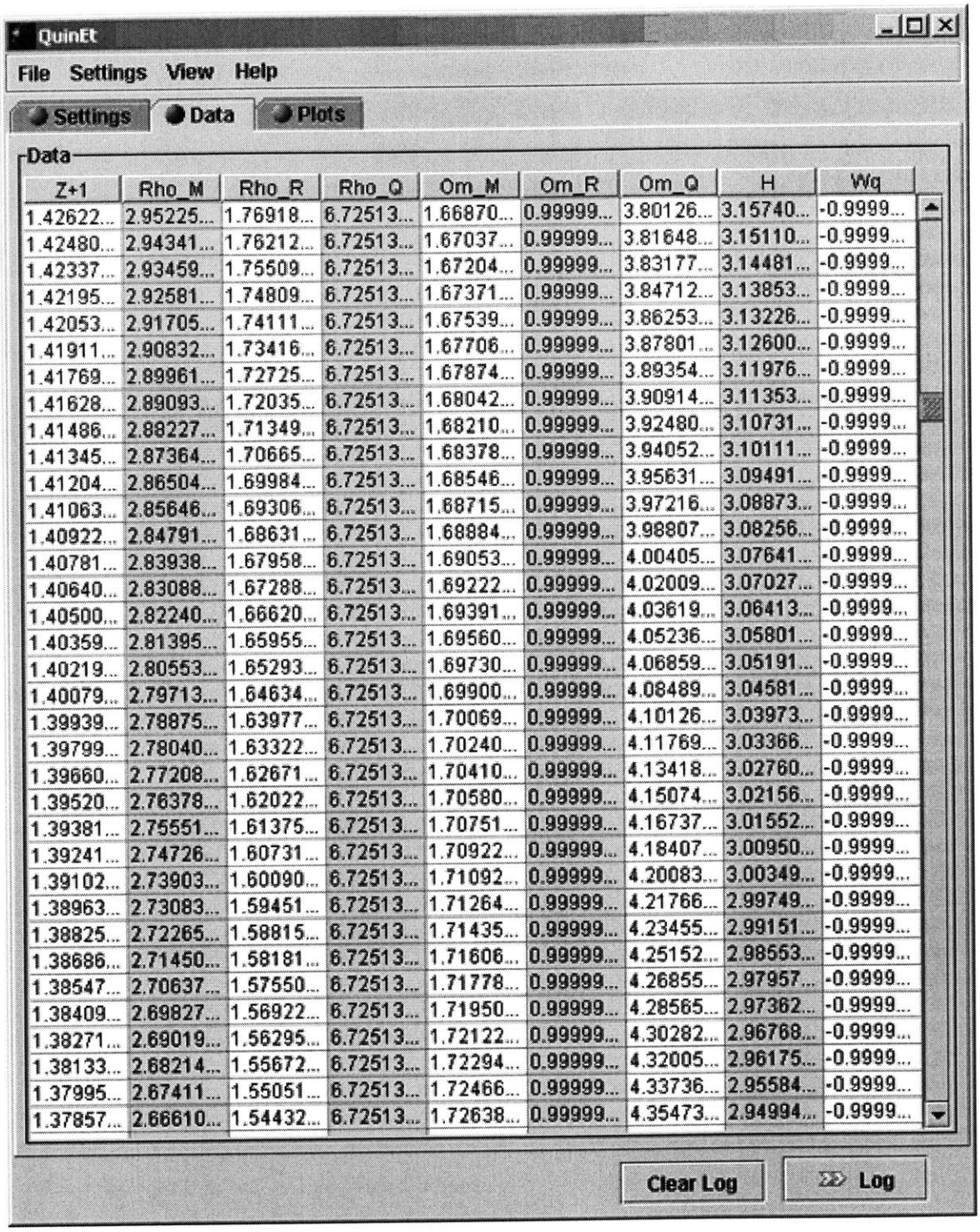


| Z+1 | Rho_M | Rho_R | Rho_Q | Om_M | Om_R | Om_Q | H | Wq |
|---|---|---|---|---|---|---|---|---|
| 1.42622... | 2.95225... | 1.76918... | 6.72513... | 1.66870... | 0.99999... | 3.80126... | 3.15740... | -0.9999... |
| 1.42480... | 2.94341... | 1.76212... | 6.72513... | 1.67037... | 0.99999... | 3.81648... | 3.15110... | -0.9999... |
| 1.42337... | 2.93459... | 1.75509... | 6.72513... | 1.67204... | 0.99999... | 3.83177... | 3.14481... | -0.9999... |
| 1.42195... | 2.92581... | 1.74809... | 6.72513... | 1.67371... | 0.99999... | 3.84712... | 3.13853... | -0.9999... |
| 1.42053... | 2.91705... | 1.74111... | 6.72513... | 1.67539... | 0.99999... | 3.86253... | 3.13226... | -0.9999... |
| 1.41911... | 2.90832... | 1.73416... | 6.72513... | 1.67706... | 0.99999... | 3.87801... | 3.12600... | -0.9999... |
| 1.41769... | 2.89961... | 1.72725... | 6.72513... | 1.67874... | 0.99999... | 3.89354... | 3.11976... | -0.9999... |
| 1.41628... | 2.89093... | 1.72035... | 6.72513... | 1.68042... | 0.99999... | 3.90914... | 3.11353... | -0.9999... |
| 1.41486... | 2.88227... | 1.71349... | 6.72513... | 1.68210... | 0.99999... | 3.92480... | 3.10731... | -0.9999... |
| 1.41345... | 2.87364... | 1.70665... | 6.72513... | 1.68378... | 0.99999... | 3.94052... | 3.10111... | -0.9999... |
| 1.41204... | 2.86504... | 1.69984... | 6.72513... | 1.68546... | 0.99999... | 3.95631... | 3.09491... | -0.9999... |
| 1.41063... | 2.85646... | 1.69306... | 6.72513... | 1.68715... | 0.99999... | 3.97216... | 3.08873... | -0.9999... |
| 1.40922... | 2.84791... | 1.68631... | 6.72513... | 1.68884... | 0.99999... | 3.98807... | 3.08256... | -0.9999... |
| 1.40781... | 2.83938... | 1.67958... | 6.72513... | 1.69053... | 0.99999... | 4.00405... | 3.07641... | -0.9999... |
| 1.40640... | 2.83088... | 1.67288... | 6.72513... | 1.69222... | 0.99999... | 4.02009... | 3.07027... | -0.9999... |
| 1.40500... | 2.82240... | 1.66620... | 6.72513... | 1.69391... | 0.99999... | 4.03619... | 3.06413... | -0.9999... |
| 1.40359... | 2.81395... | 1.65955... | 6.72513... | 1.69560... | 0.99999... | 4.05236... | 3.05801... | -0.9999... |
| 1.40219... | 2.80553... | 1.65293... | 6.72513... | 1.69730... | 0.99999... | 4.06859... | 3.05191... | -0.9999... |
| 1.40079... | 2.79713... | 1.64634... | 6.72513... | 1.69900... | 0.99999... | 4.08489... | 3.04581... | -0.9999... |
| 1.39939... | 2.78875... | 1.63977... | 6.72513... | 1.70069... | 0.99999... | 4.10126... | 3.03973... | -0.9999... |
| 1.39799... | 2.78040... | 1.63322... | 6.72513... | 1.70240... | 0.99999... | 4.11769... | 3.03366... | -0.9999... |
| 1.39660... | 2.77208... | 1.62671... | 6.72513... | 1.70410... | 0.99999... | 4.13418... | 3.02760... | -0.9999... |
| 1.39520... | 2.76378... | 1.62022... | 6.72513... | 1.70580... | 0.99999... | 4.15074... | 3.02156... | -0.9999... |
| 1.39381... | 2.75551... | 1.61375... | 6.72513... | 1.70751... | 0.99999... | 4.16737... | 3.01552... | -0.9999... |
| 1.39241... | 2.74726... | 1.60731... | 6.72513... | 1.70922... | 0.99999... | 4.18407... | 3.00950... | -0.9999... |
| 1.39102... | 2.73903... | 1.60090... | 6.72513... | 1.71092... | 0.99999... | 4.20083... | 3.00349... | -0.9999... |
| 1.38963... | 2.73083... | 1.59451... | 6.72513... | 1.71264... | 0.99999... | 4.21766... | 2.99749... | -0.9999... |
| 1.38825... | 2.72265... | 1.58815... | 6.72513... | 1.71435... | 0.99999... | 4.23455... | 2.99151... | -0.9999... |
| 1.38686... | 2.71450... | 1.58181... | 6.72513... | 1.71606... | 0.99999... | 4.25152... | 2.98553... | -0.9999... |
| 1.38547... | 2.70637... | 1.57550... | 6.72513... | 1.71778... | 0.99999... | 4.26855... | 2.97957... | -0.9999... |
| 1.38409... | 2.69827... | 1.56922... | 6.72513... | 1.71950... | 0.99999... | 4.28565... | 2.97362... | -0.9999... |
| 1.38271... | 2.69019... | 1.56295... | 6.72513... | 1.72122... | 0.99999... | 4.30282... | 2.96768... | -0.9999... |
| 1.38133... | 2.68214... | 1.55672... | 6.72513... | 1.72294... | 0.99999... | 4.32005... | 2.96175... | -0.9999... |
| 1.37995... | 2.67411... | 1.55051... | 6.72513... | 1.72466... | 0.99999... | 4.33736... | 2.95584... | -0.9999... |
| 1.37857... | 2.66610... | 1.54432... | 6.72513... | 1.72638... | 0.99999... | 4.35473... | 2.94994... | -0.9999... |

Figure 3-7: Data from calculation or imported from file can be directly displayed and edited. Data from this view can also be saved by first selecting specific columns—to select multiple columns, press and hold the "Control" key while selecting cells of different column—and selecting "Save data" from the "File" menu.

### 3.2.3 Plot

The plot component is the most elaborately designed aspect of QuintET. As discussed below, this component has interfaces for zooming in and out, dragging the axes, labeling, sampling of data, and many more. The tick mark values are *intelligently* calculated to display meaningful numbers. This becomes more complicated since axes reversing as well as log–linear plotting is supported (see figure (3-9)).

Right–click on the drawing area gives a pop–up window that has a number of useful tools. The first two tools, which are mutually exclusive, enable the dragging and zooming capabilities. These features are designed to be error tolerant as a number of unwanted and often unexpected results can happen (out–of–bounds errors for example). Following these is the `Zoom Level`, which extends to give a multiple selection that change the effect of clicking on the drawing area. `Add Text`, `Clear Last Text` and `Clear All Text` deal with labeling and adding text to the plot. The following is a brief discussion of each of these features (see figure (3-10)).

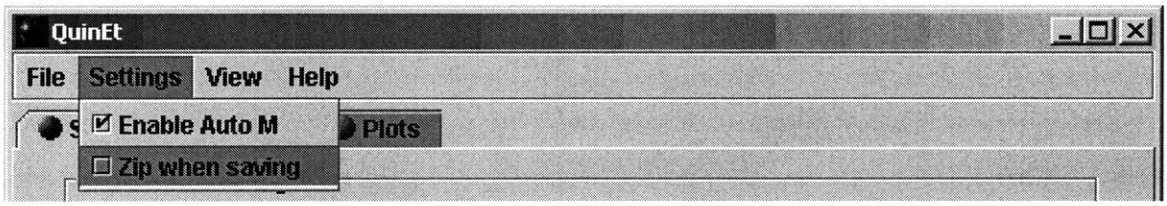


Figure 3-8: If the `Zip when saving` option is selected, saved data file is zipped.

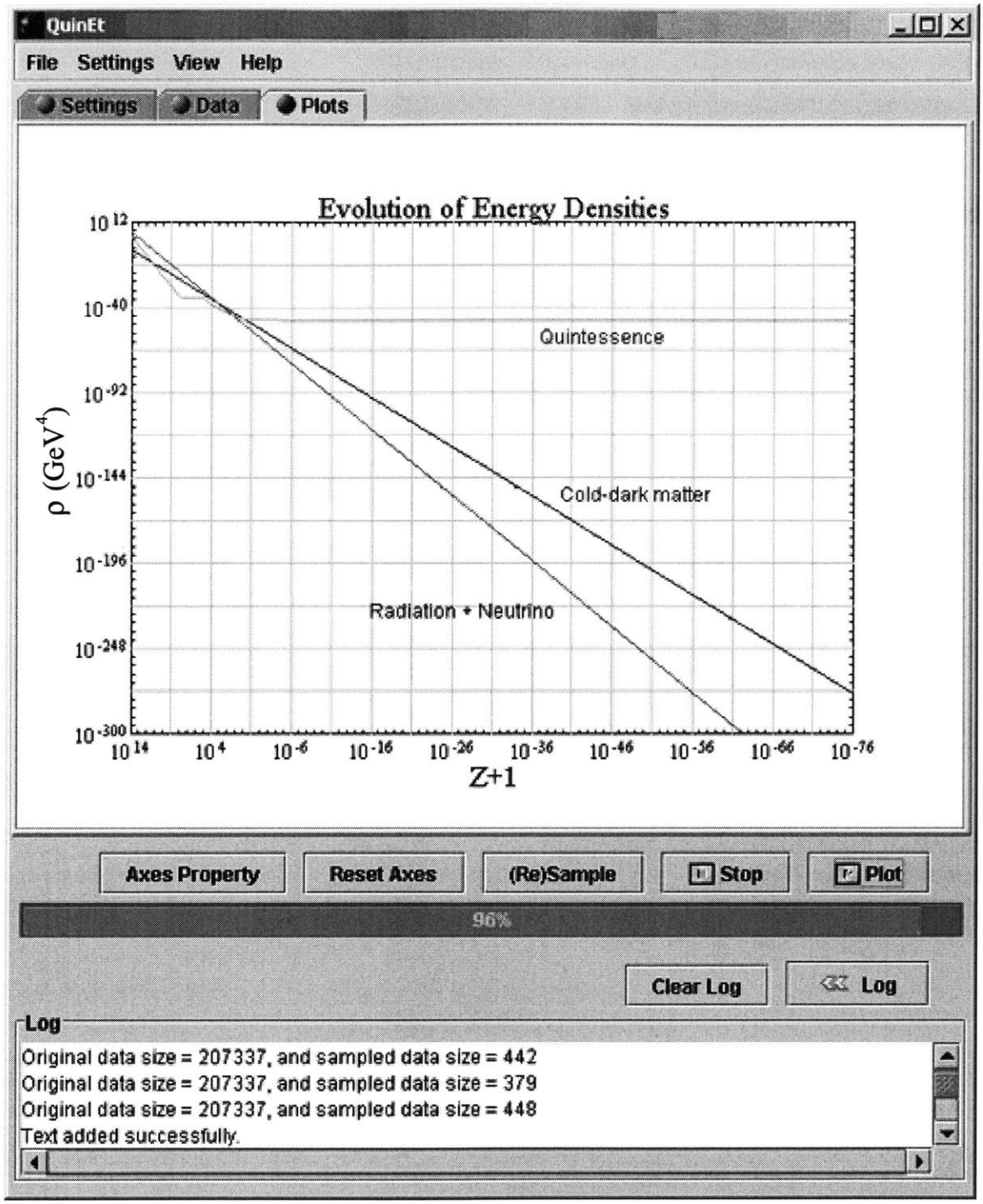


Figure 3-9: The plotting interface allows for zooming in and out, dragging the axes, labeling, etc.

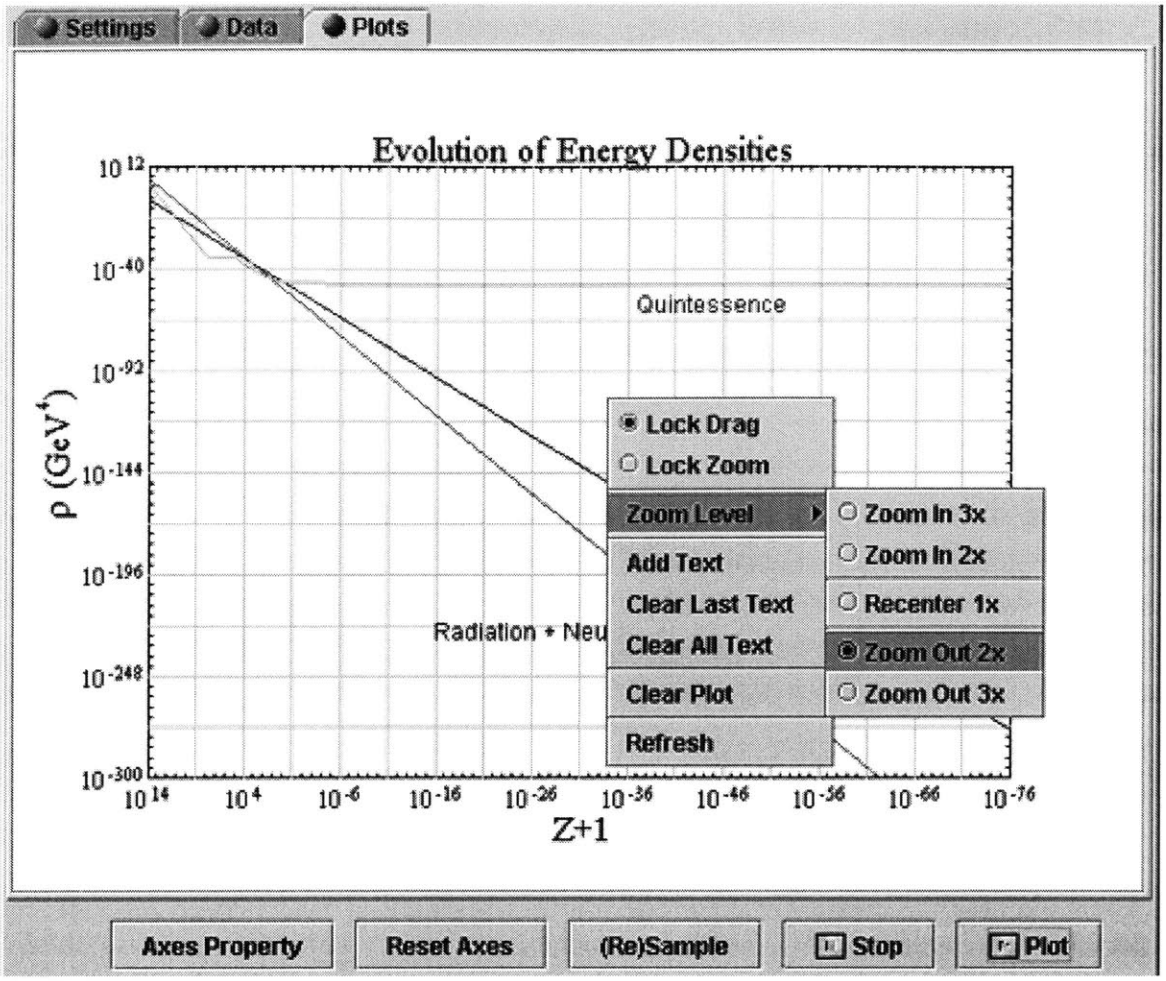


Figure 3-10: Right–click on the plotting area reveals a pop–up menu with a number of tools such as selecting either the drag or zoom mode, selecting a zooming level and labeling tools.

### Dragging

If `Lock Drag` is selected, clicking and dragging the mouse drags the drawing area along with it. This is very convenient as it allows the user to quickly navigate the plot to see a specific feature or part of the plot.

### Zooming

Zooming, via zoom–box or scaling of the current plot is possible by enabling the `Lock Zoom` or choosing from the different `Zoom Levels`, respectively (see figure (3-10)). If `Lock Zoom` is enabled, a left mouse click and subsequent dragging of the mouse while

the button is still pressed displays a zoom–box (a rectangular area) with one vertex at the position of the initial click and the diagonally opposite vertex at the current position of the mouse. If the button is released, the current drawing area axes limits are set to reflect the zoom–box dimension and location. This features is very powerful as it allows for a very precise view of the plot under investigation (see figure (3-11)).

Alternatively, if anyone of the five selections under `Zoom Level` are selected, a single click on any part of the plot will, first, make the click–point to be the center of the plot and, secondly, the plot will be scaled according to the selected level. If the selected level has a scale factor of one, then the plot simply re-centers without scaling.

### Text and Label

Text and labels can be added anywhere in the drawing area. Specifically, $x$ and $y$ labels can be added and a title can be set using the `Add Text` tool in the pop–up (figure (3-10)) menu. The $x$ and $y$ coordinates of the left–top corner of the text to be displayed is set by default to be the location of the pop–up. This value, however, can be changed at will from the`Add Text` interface. Resizing the window does not alter where the text is placed, and furthermore the labels and title are always placed in the correct place regardless what values of $x$ and $y$ are set in the interface. The last text to be added (regardless if it is a title, label or just text) could be recursively removed, or alternatively the plot can be cleared off all text by selecting the appropriate button from the pop–up. See figure (3-12).

### Axes Property

Axes setting is another comprehensive design in QuintET. All the basic features of plotting found in many data visualization tools are supported. The Axes Property window is displayed when the corresponding button is clicked (see figure (3-13). Therein, the scale, data source and $(x, y)$ data, for multiple $(x, y)$s, are specified. Either axis can have a grid, and the limits can be reversed and the scale can either be log or linear. Data source can either be from the latest calculation (and the selected

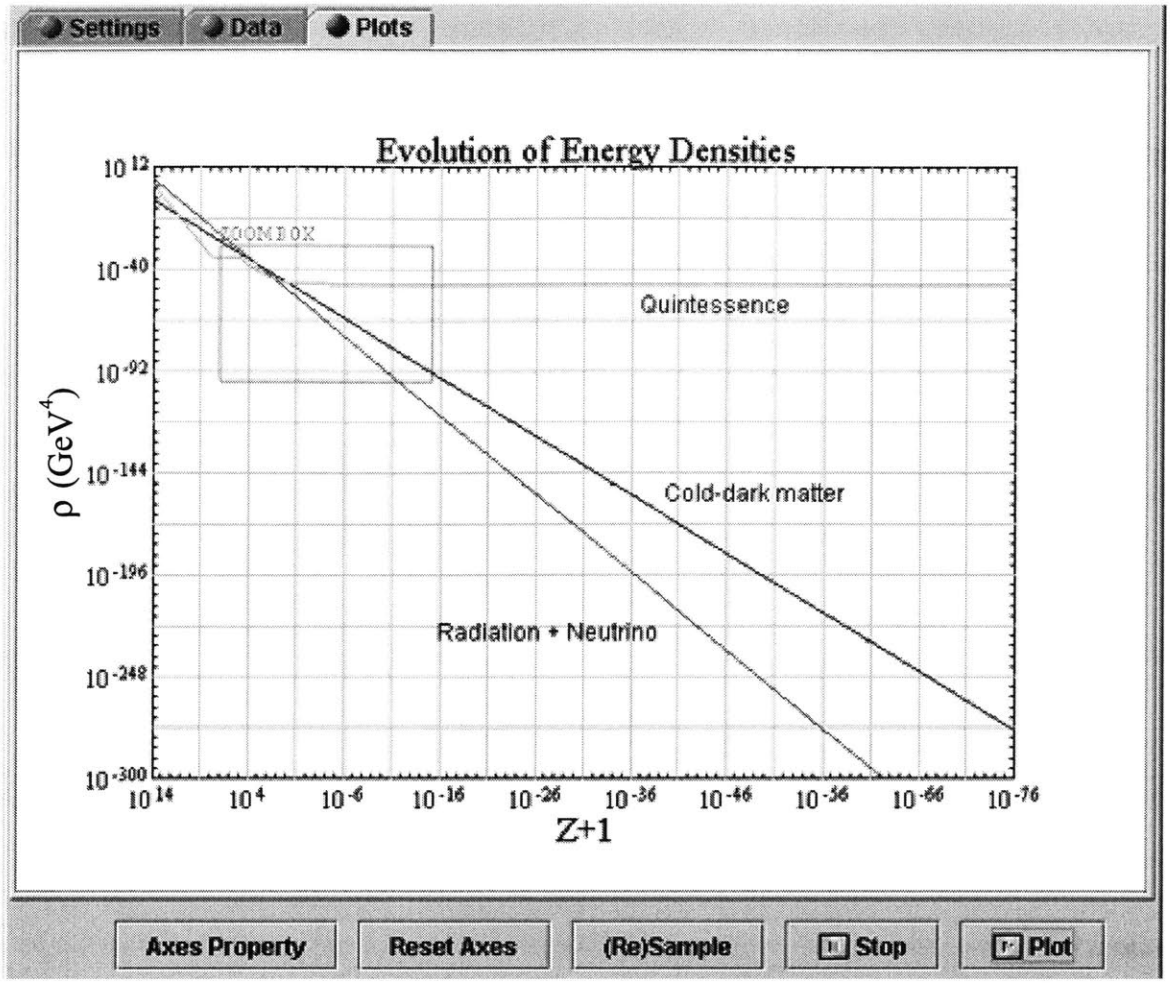


Figure 3-11: In zooming mode, if a mouse is dragged after being clicked (and held clicked) within the drawing area, a rectangular box (the zoom–box) is displayed. Upon release of the mouse, the dimensions of the drawing area reflect that of the zoom–box.

parameters are automatically loaded in the drop–down menu for each axis) or from an imported data set. The `Add>>` button adds the selected $(x, y)$ parameter in the list of to be plotted parameters. `Remove All` removes all parameters that have been selected to be plotted, and `Clear` only removes the recently added parameters to the list.

### Data Sampling

Once the data is selected, it is not plotted right away (nor could it be plotted). It is often the case that the data contains far more data points than what the current

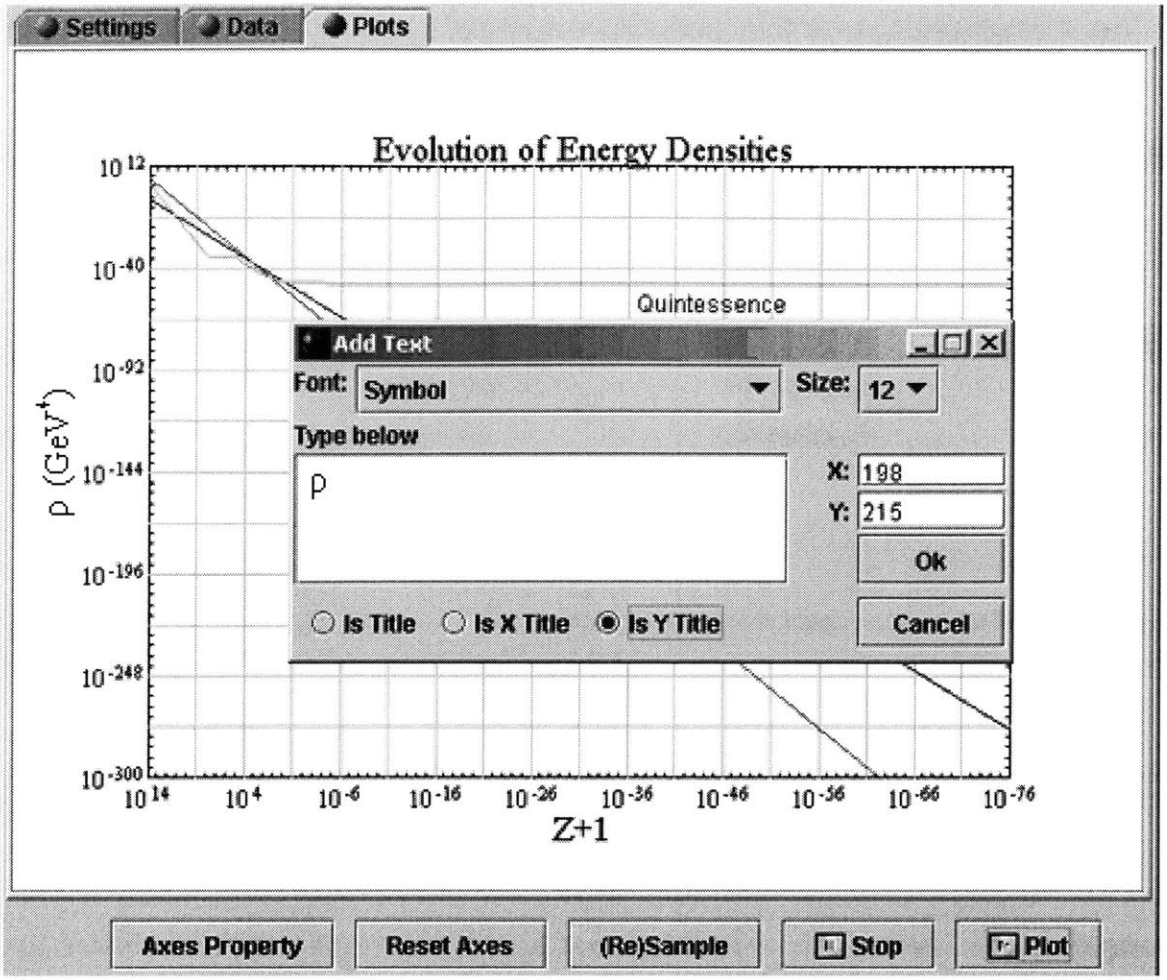


Figure 3-12: The `Add Text` interface. The font, size, location and whether the text is a label, title is specified here.

display resolution of the monitor could handle. All data sources must first be sampled according to a density factor that is specific to the height and width of the current plotting area. Without sampling and for a very dense data, plotting time takes too long and dragging and zooming becomes a time consuming procedure with limited benefit. Hence, sampling is enforced for all data source, and each data source must be of the allowed format for this to take place.

### Saving Plot

Saving a plot is straightforward. All saved plots are in PostScript format. The saving algorithm attempts to do a better job than "what you see is what you get" approach

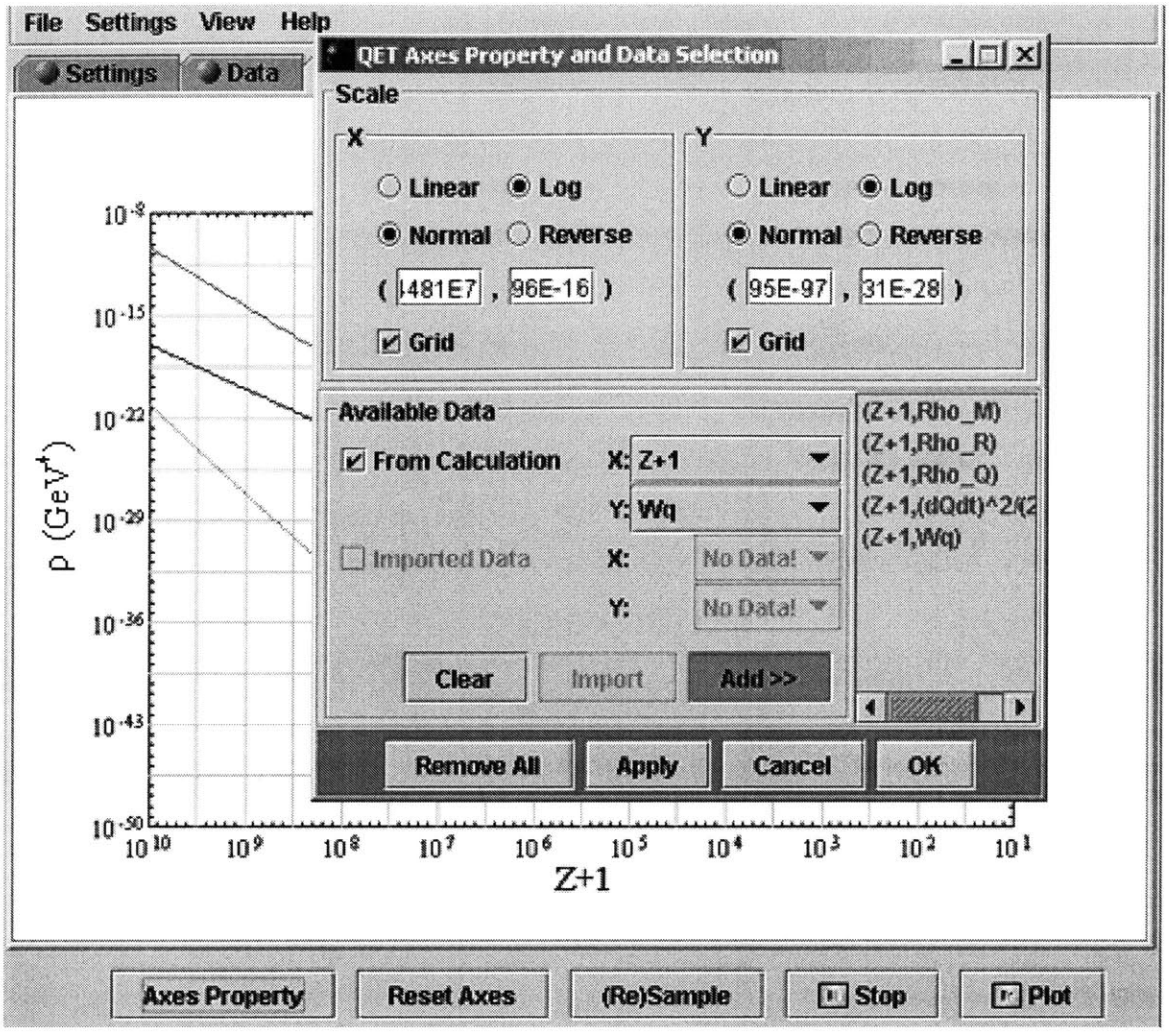


Figure 3-13: Here the axes properties are set. `Scale` corresponds to the limit, scale, normal–reverse and grid settings while `Available Data` corresponds to the overall available data and the selected subset.

by scaling and resampling the data to allow for the most crisp PostScript output.

### 3.2.4 Miscellaneous

A few items that need a brief discussion are the Menus and the Log component.

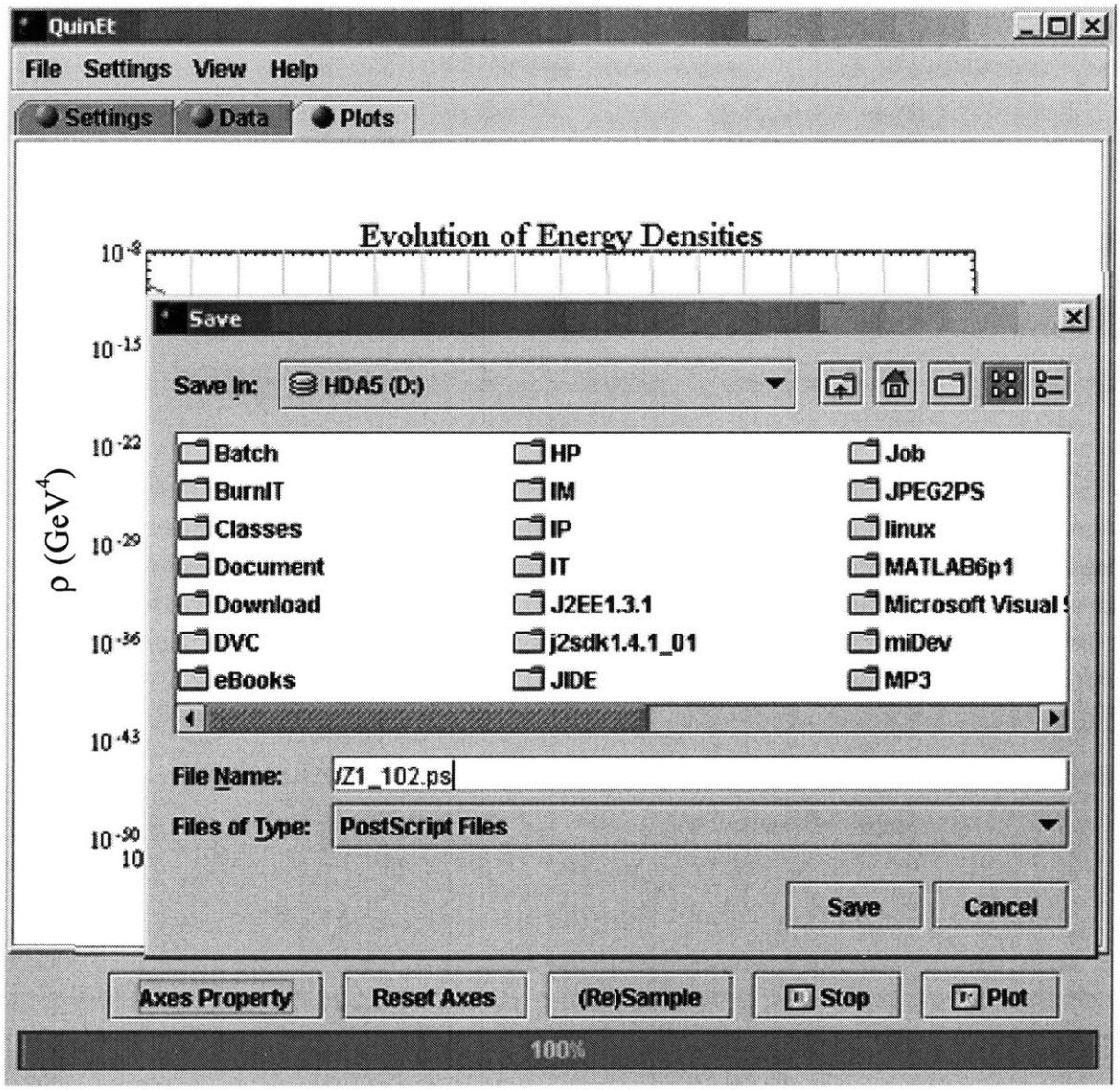


Figure 3-14: Saving plot.

### Menu

The menus, see figures (3-15), (3-16), (3-8), (3-17) and (3-18), have access to some settings as well as access to the help file. Print preview, page setup, zip when saving data option, font setting, etc. are accessed from these menus.

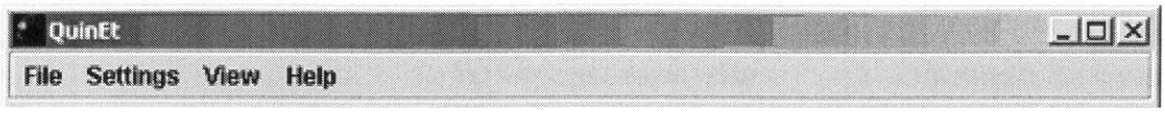


Figure 3-15: The QuintET menu interface.

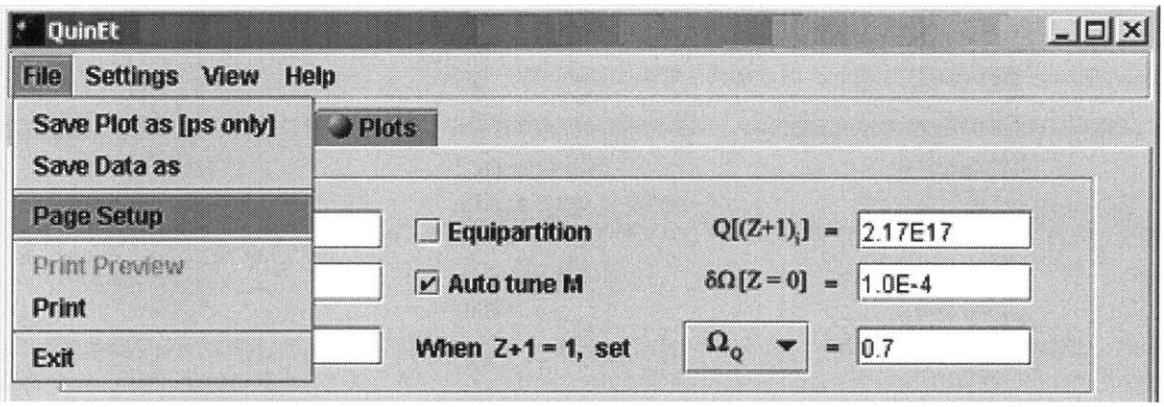


Figure 3-16: The `File` menu.

### Log

The Log, accessible from the calculation, data and plot components, displays any errors from subprocesses or/and user input. It can be enabled and disabled at will using the button provided. The Log also accepts keyboard input and can be saved to file from the File menu.

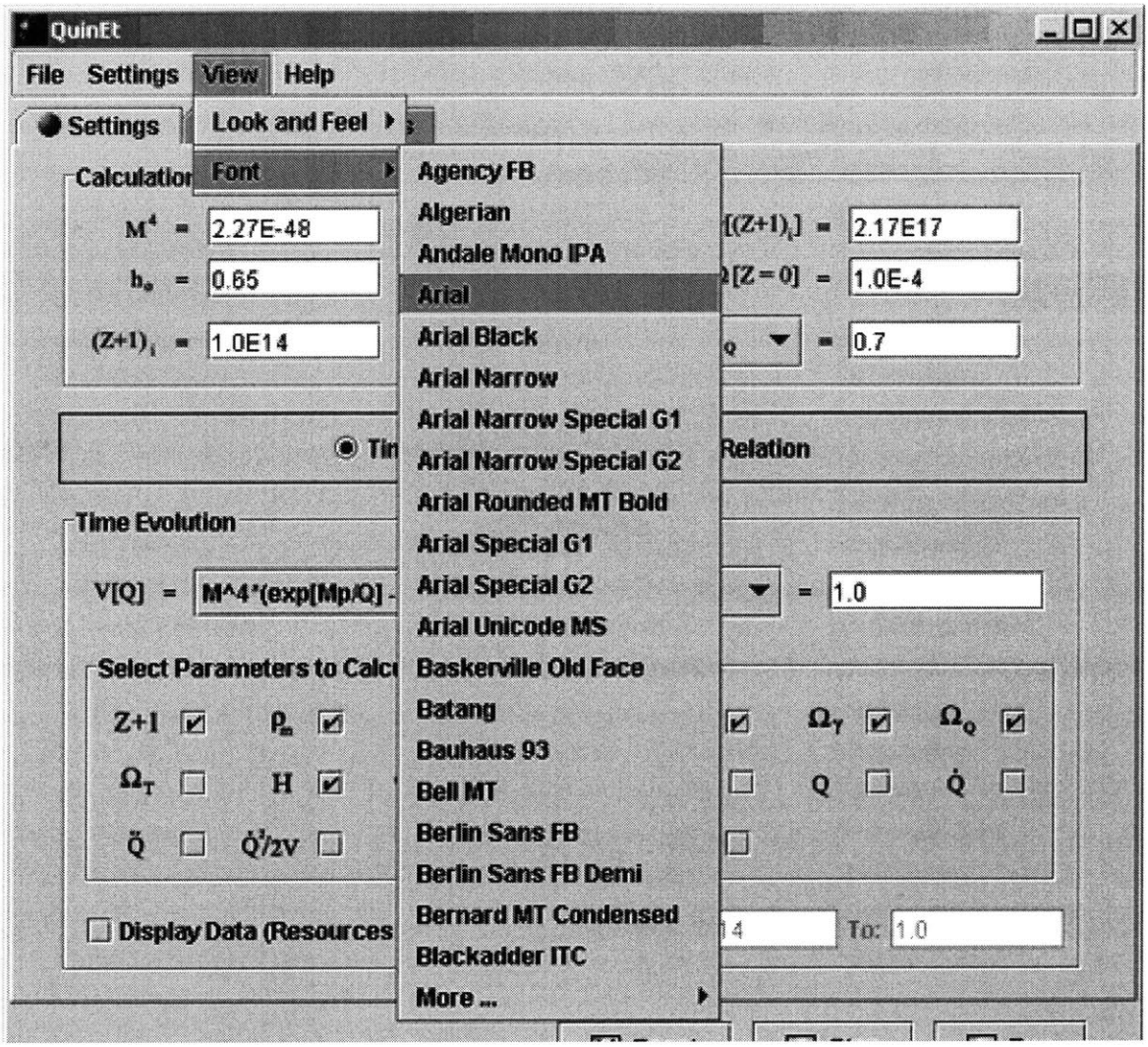


Figure 3-17: The `View` menu.

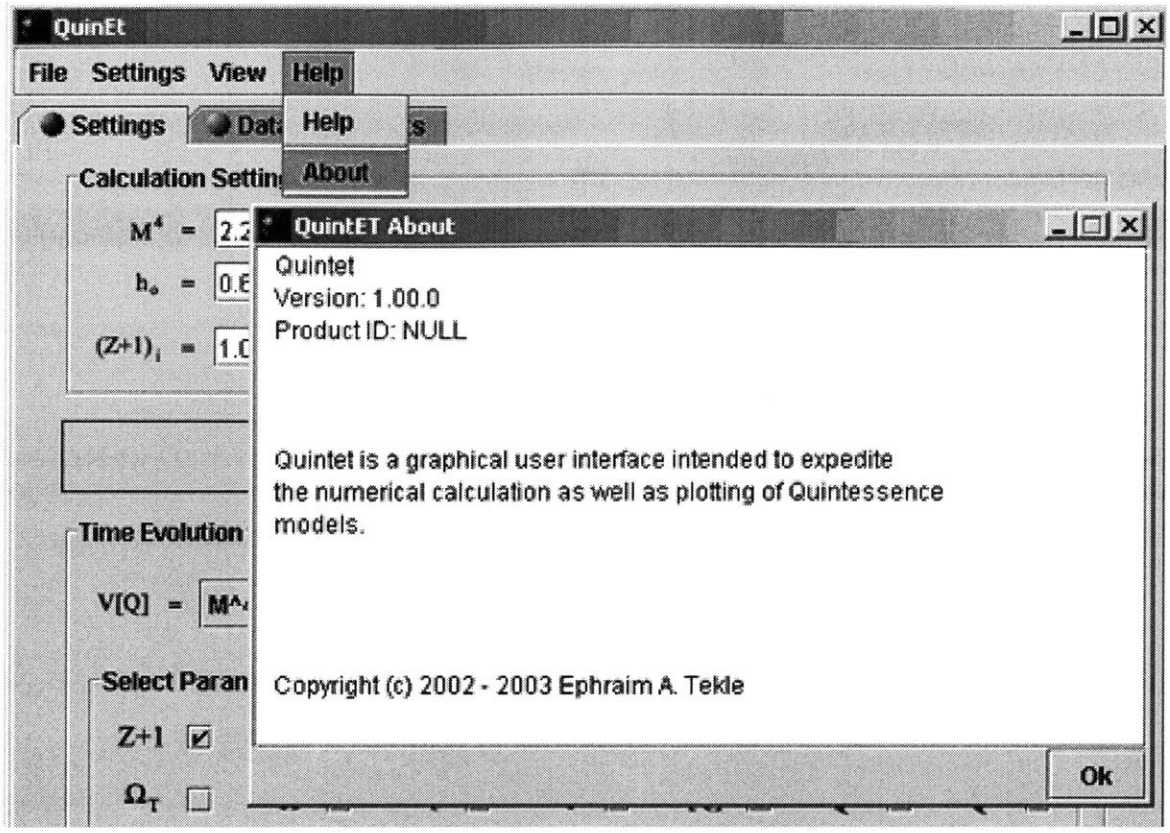


Figure 3-18: The help menu.

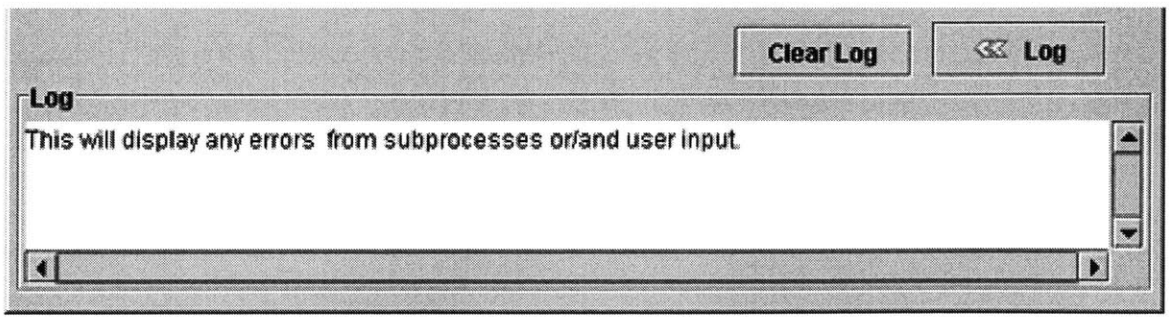


Figure 3-19: Errors from subprocesses or/and user input log.

## 3.3 Future Work

More work needs to be done to increase the versatility of QuintET. In line with the modularity requirements, additional components can be added for more sophisticated numerical calculations. Support for multi–format import/export of diagrams and data is also the next target in the development of QuintET.

# Chapter 4

# Conclusion

The development of QuintET took roughly 5 months. During this time, the requirements have changed a number of times. The initial requirement was narrowly focused on the numerical calculation part, with data visualization done using Matlab. Overtime, however, it was realized that the benefit of having an integrated data visualization tool justifies the effort.

In Object Oriented development, building user interfaces becomes considerably simplified. However, a sound and efficient algorithm to handle the real task (numerical integration in this case) is often not given adequate time and thinking. In the development of QuintET, this issue was addressed by the overall structure of the user interface, and also by the algorithm developed to handle heavily coupled partial differential equations.

# Appendix A

# Scalar Field–Curvature Coupling

Herein is presented complete derivation, without any restriction on the underlining space–time, of the solutions to Albert Einstein's field equations. Important final results are placed inside a box

In the study of scalar field cosmologies, it is very important to study if there is any significant coupling between scalar fields and gravity. Coupling term such as $\frac{1}{2}\xi\phi^2 R$ (non–minimal coupling) is not excluded theoretically, and since the coupling gives rise to observational effects, the strength of the coupling parameter, $\xi$, can be constrained by observation.

Starting from the action

$$\begin{aligned} S &= \int d^4x\sqrt{-g}\left[\frac{R}{2\kappa} - \frac{1}{2}\xi\phi^2 R - \left\{\frac{1}{2}g^{\mu\nu}\partial_\mu\phi\partial_\nu\phi + V(\phi)\right\}\right] + S_B \\ &= \int d^4x\sqrt{-g}\left[\left(\frac{1}{2\kappa} - \frac{1}{2}\xi\phi^2\right)R - \left\{\frac{1}{2}g^{\mu\nu}\partial_\mu\phi\partial_\nu\phi + V(\phi)\right\}\right] + S_B \\ &= \int d^4x\sqrt{-g}\left[f(\phi)R - \left\{\frac{1}{2}g^{\mu\nu}\partial_\mu\phi\partial_\nu\phi + V(\phi)\right\}\right] + S_B, \text{ where} \qquad \text{(A.1)} \\ f(\phi) &\equiv \frac{1}{2\kappa}\left(1 - \xi\kappa\phi^2\right), \ \kappa = 8\pi G, \qquad \text{(A.2)} \end{aligned}$$

$R$ is the Ricci scalar curvature, $R = g^{\mu\nu}R_{\mu\nu}$, and $S_B$ denotes the action of the *background* matter.

Setting the variation of the action, $S$, to zero,

$$\delta S = 0, \tag{A.3}$$

the first part of the integral (A.1) gives

$$\begin{aligned}
\delta \int d^4x\sqrt{-g}f(\phi)R &= \delta \int d^4x\sqrt{-g}g^{\mu\nu}R_{\mu\nu}f(\phi) \\
&= \int d^4x\sqrt{-g}f(\phi)g^{\mu\nu}\delta R_{\mu\nu} + \int d^4x f(\phi)R_{\mu\nu}\delta\left(\sqrt{-g}g^{\mu\nu}\right) \\
&\quad + \int d^4x\sqrt{-g}g^{\mu\nu}R_{\mu\nu}\delta f(\phi).
\end{aligned} \tag{A.4}$$

Using the geodesic coordinate system to obtain $\delta R_{\mu\nu}$, it follows

$$\begin{aligned}
\delta R_{\mu\nu} &= \delta\left[\partial_\rho\Gamma^\rho_{\mu\nu} - \partial_\nu\Gamma^\rho_{\mu\rho} + \Gamma^\sigma_{\mu\nu}\Gamma^\rho_{\rho\sigma} - \Gamma^\sigma_{\mu\rho}\Gamma^\rho_{\nu\sigma}\right] \\
&= \delta\left[\partial_\rho\Gamma^\rho_{\mu\nu} - \partial_\nu\Gamma^\rho_{\mu\rho}\right], \text{ since } \delta\partial = \partial\delta, \\
&= \partial_\rho\left(\delta\Gamma^\rho_{\mu\nu}\right) - \partial_\nu\left(\delta\Gamma^\rho_{\mu\rho}\right) \\
&= \nabla_\rho\left(\delta\Gamma^\rho_{\mu\nu}\right) - \nabla_\nu\left(\delta\Gamma^\rho_{\mu\rho}\right),
\end{aligned} \tag{A.5}$$

where the last step follows directly from the definition of covariant derivative. For any vector $V_\nu$, for example, one obtains

$$\nabla_\mu V_\nu - \nabla_\nu V_\mu = \partial_\mu V_\nu - \partial_\nu V_\mu.$$

Since equation (A.5) is coordinate independent, the integrand of the first integral on the right-hand side of equation(A.4) can be written as,

$$\begin{aligned}
\sqrt{-g}f(\phi)g^{\mu\nu}\delta R_{\mu\nu} &= \sqrt{-g}f(\phi)g^{\mu\nu}\left\{\nabla_\rho\left(\delta\Gamma^\rho_{\mu\nu}\right) - \nabla_\nu\left(\delta\Gamma^\rho_{\mu\rho}\right)\right\}, \text{ and since } \nabla_\alpha g^{\mu\nu} = 0 \\
&= \sqrt{-g}f(\phi)\left\{\nabla_\rho\left(g^{\mu\nu}\delta\Gamma^\rho_{\mu\nu}\right) - \nabla_\nu\left(g^{\mu\nu}\delta\Gamma^\rho_{\mu\rho}\right)\right\} \\
&= \sqrt{-g}f(\phi)\left\{\nabla_\alpha\left(g^{\mu\nu}\delta\Gamma^\alpha_{\mu\nu}\right) - \nabla_\alpha\left(g^{\mu\alpha}\delta\Gamma^\rho_{\mu\rho}\right)\right\} \\
&= \sqrt{-g}f(\phi)\nabla_\alpha V^\alpha,
\end{aligned} \tag{A.6}$$

where

$$V^\alpha \equiv g^{\mu\nu}\delta\Gamma^\alpha_{\mu\nu} - g^{\mu\alpha}\delta\Gamma^\rho_{\mu\rho}.$$

Using the relation $dg = gg^{\mu\nu}dg_{\mu\nu}$ and by contracting a pair of indices of the Christoffel symbols, one obtains

$$\begin{aligned}\Gamma^\mu_{\rho\mu} &= g^{\mu\nu}\Gamma_{\nu\rho\mu} = \frac{1}{2}g^{\mu\nu}\partial_\rho g_{\mu\nu} \\ &= \frac{1}{2g}\partial_\rho g = \frac{1}{\sqrt{-g}}\partial_\rho\sqrt{-g}. \end{aligned} \tag{A.7}$$

With the above result, the covariant divergence of a vector $V^\mu$ can be written as

$$\nabla_\mu V^\mu = \partial_\mu V^\mu + \Gamma^\mu_{\alpha\mu}V^\alpha = \frac{1}{\sqrt{-g}}\partial_\mu\left(\sqrt{-g}V^\mu\right). \tag{A.8}$$

Consequently, using equations (A.6), (A.7) and (A.8), the first integral on the right-hand side of equation (A.4) can be rewritten as

$$\begin{aligned}\int d^4x\sqrt{-g}f(\phi)g^{\mu\nu}\delta R_{\mu\nu} &= \int d^4x f(\phi)\partial_\alpha\left(\sqrt{-g}V^\alpha\right), \text{ and using integration by parts} \\ &= \int d^4x\partial_\alpha\left\{f(\phi)\sqrt{-g}V^\alpha\right\} - \int d^4x\sqrt{-g}V^\alpha\partial_\alpha f(\phi) \\ &= -\int d^4x\sqrt{-g}V^\alpha\partial_\alpha f(\phi) + (\text{vanishing surface term}) \\ &= \int d^4x\sqrt{-g}g^{\mu\alpha}\delta\Gamma^\rho_{\mu\rho}\partial_\alpha f(\phi) - \int d^4x\sqrt{-g}g^{\mu\nu}\delta\Gamma^\alpha_{\mu\nu}\partial_\alpha f(\phi) \end{aligned} \tag{A.9}$$

From equation(A.7) and the relation $dg = gg^{\mu\nu}dg_{\mu\nu}$ and , $\delta\Gamma^\rho_{\mu\rho}$ can be rewritten as

$$\begin{aligned}\delta\Gamma^\rho_{\mu\rho} &= \partial_\mu\sqrt{-g}\delta\left(\frac{1}{\sqrt{-g}}\right) + \frac{1}{\sqrt{-g}}\partial_\mu\left(\delta\sqrt{-g}\right) \\ &= \frac{1}{2\sqrt{-g}}\partial_\mu\sqrt{-g}g_{\rho\alpha}\delta g^{\rho\alpha} + \frac{1}{\sqrt{-g}}\partial_\mu\left(\delta\sqrt{-g}\right). \end{aligned} \tag{A.10}$$

With this result, the first integral on the right-hand side of equation (A.9) can be

expressed as

$$\int d^4x\sqrt{-g}g^{\mu\alpha}\delta\Gamma^{\rho}_{\mu\rho}\partial_\alpha f(\phi) = \int d^4x\sqrt{-g}\left\{\frac{1}{2\sqrt{-g}}g_{\mu\nu}g^{\rho\alpha}\partial_\alpha f(\phi)\partial_\rho\sqrt{-g}\right\}\delta g^{\mu\nu} + \int d^4x g^{\rho\alpha}\partial_\alpha f(\phi)\partial_\rho\left(\delta\sqrt{-g}\right). \quad \text{(A.11)}$$

Using integration by parts, the second integral on the right-hand side of equation (A.11) can be written as

$$\int d^4x g^{\rho\alpha}\partial_\alpha f(\phi)\partial_\rho\left(\delta\sqrt{-g}\right) = \int d^4x\partial_\rho\left(g^{\rho\alpha}\partial_\alpha f(\phi)\delta\sqrt{-g}\right) - \int d^4x\partial_\rho\left(g^{\rho\alpha}\partial_\alpha f\right)\delta\sqrt{-g} = \int d^4x\sqrt{-g}\left\{\frac{1}{2}\partial_\rho\left(g^{\rho\alpha}\partial_\alpha f\right)g_{\mu\nu}\right\}\delta g^{\mu\nu} + (\text{vanishing surface term}) \quad \text{(A.12)}$$

Putting equations (A.11) and (A.12) together, the first integral on the right-hand side of equation (A.9) becomes,

$$\int d^4x\sqrt{-g}g^{\mu\alpha}\delta\Gamma^{\rho}_{\mu\rho}\partial_\alpha f(\phi) = \int d^4x\sqrt{-g}\left\{\frac{1}{2\sqrt{-g}}g_{\mu\nu}g^{\rho\alpha}\partial_\alpha f(\phi)\partial_\rho\sqrt{-g} + \frac{1}{2}\partial_\rho\left(g^{\rho\alpha}\partial_\alpha f\right)g_{\mu\nu}\right\}\delta g^{\mu\nu} = \int d^4x\sqrt{-g}\left(-\frac{1}{2}T^1_{\mu\nu}\right)\delta g^{\mu\nu}, \quad \text{(A.13)}$$

where $T^1_{\mu\nu}$ is defined as

$$\boxed{T^1_{\mu\nu} \equiv -\left[\frac{1}{\sqrt{-g}}g^{\rho\alpha}\partial_\alpha f(\phi)\partial_\rho\sqrt{-g} + \partial_\rho\left(g^{\rho\alpha}\partial_\alpha f\right)\right]g_{\mu\nu}}. \quad \text{(A.14)}$$

The second integral on the right hand side of equation (A.9) can be simplified by rewriting $-g^{\mu\nu}\delta\Gamma^{\alpha}_{\mu\nu}$ as,

$$-g^{\mu\nu}\delta\Gamma^{\alpha}_{\mu\nu} = -\delta\left(g^{\mu\nu}\Gamma^{\alpha}_{\mu\nu}\right) + \Gamma^{\alpha}_{\mu\nu}\delta g^{\mu\nu}, \text{ therefore}$$

$$-\int d^4x\sqrt{-g}g^{\mu\nu}\delta\Gamma^{\alpha}_{\mu\nu}\partial_\alpha f(\phi) = \int d^4x\sqrt{-g}\left\{\Gamma^{\alpha}_{\mu\nu}\partial_\alpha f(\phi)\right\}\delta g^{\mu\nu} - \int d^4x\sqrt{-g}\partial_\alpha f(\phi)\delta\left(g^{\mu\nu}\Gamma^{\alpha}_{\mu\nu}\right). \quad \text{(A.15)}$$

The integrand of the second integral on the right-hand side of equation (A.15) can

be simplified by noticing that

$$\begin{aligned} g^{\mu\nu}\Gamma^{\alpha}_{\mu\nu} &= \frac{1}{2}g^{\mu\nu}g^{\alpha\rho}\left(\partial_\nu g_{\rho\mu} + \partial_\mu g_{\rho\nu} - \partial_\rho g_{\mu\nu}\right) \\ &= g^{\mu\nu}g^{\alpha\rho}\left(\partial_\nu g_{\rho\mu} - \frac{1}{2}\partial_\rho g_{\mu\nu}\right), \text{ using } \begin{cases} g^{\mu\nu}g^{\alpha\rho}\partial_\nu g_{\rho\mu} = -\partial_\nu g^{\alpha\nu} \\ \text{and equation (A.7)} \end{cases} \\ &= -\frac{1}{\sqrt{-g}}\partial_\nu\left\{\sqrt{-g}g^{\alpha\nu}\right\}. \end{aligned} \tag{A.16}$$

Finally, using the relation $dg = gg^{\mu\nu}dg_{\mu\nu}$ and equation(A.16),

$$\begin{aligned} -\delta\left(g^{\mu\nu}\Gamma^{\alpha}_{\mu\nu}\right) &= \partial_\nu\left\{\sqrt{-g}g^{\alpha\nu}\right\}\delta\left(\frac{1}{\sqrt{-g}}\right) + \frac{1}{\sqrt{-g}}\delta\partial_\nu\left\{\sqrt{-g}g^{\alpha\nu}\right\} \\ &= \frac{1}{2\sqrt{-g}}\partial_\rho\left\{\sqrt{-g}g^{\alpha\rho}\right\}g_{\mu\nu}\delta g^{\mu\nu} + \frac{1}{\sqrt{-g}}\partial_\nu\left\{\delta\left[\sqrt{-g}g^{\alpha\nu}\right]\right\} \end{aligned} \tag{A.17}$$

With this result, the second integral on the right-hand side of equation (A.15) becomes

$$\begin{aligned} -\int d^4x\sqrt{-g}\partial_\alpha f(\phi)\delta\left(g^{\mu\nu}\Gamma^{\alpha}_{\mu\nu}\right) &= \int d^4x\sqrt{-g}\left\{\frac{1}{2\sqrt{-g}}g_{\mu\nu}\partial_\rho\left[\sqrt{-g}g^{\alpha\rho}\right]\partial_\alpha f(\phi)\right\}\delta g^{\mu\nu} \\ &\quad + \int d^4x\partial_\alpha f(\phi)\partial_\nu\left\{\delta\left[\sqrt{-g}g^{\alpha\nu}\right]\right\}. \end{aligned} \tag{A.18}$$

Using integration by parts, the second integral on the right-hand side of equation (A.18) becomes

$$\begin{aligned} \int d^4x\partial_\alpha f(\phi)\partial_\nu\left\{\delta\left[\sqrt{-g}g^{\alpha\nu}\right]\right\} &= \int d^4x\partial_\nu\left\{\partial_\alpha f(\phi)\delta\left[\sqrt{-g}g^{\alpha\nu}\right]\right\} - \int d^4x\partial_\nu\partial_\alpha f(\phi)\delta\left[\sqrt{-g}g^{\alpha\nu}\right] \\ &= -\int d^4x\partial_\nu\partial_\alpha f(\phi)\delta\left[\sqrt{-g}g^{\alpha\nu}\right] + (\text{vanishing surface term}) \\ &= -\int d^4x\partial_\rho\partial_\alpha f(\phi)g^{\alpha\rho}\delta\sqrt{-g} - \int d^4x\partial_\mu\partial_\nu f(\phi)\sqrt{-g}\delta g^{\mu\nu} \\ &= \int d^4x\sqrt{-g}\left\{\frac{1}{2}g_{\mu\nu}g^{\alpha\rho}\partial_\rho\partial_\alpha f(\phi)\right\}\delta g^{\mu\nu} \\ &\quad - \int d^4x\sqrt{-g}\left\{\partial_\mu\partial_\nu f(\phi)\right\}\delta g^{\mu\nu}. \end{aligned} \tag{A.19}$$

Putting equations (A.15), (A.18) and (A.19) together, the second integral on the

right-hand side of equation (A.9) becomes

$$
\begin{aligned}
-\int d^4x\sqrt{-g}g^{\mu\nu}\delta\Gamma^{\alpha}_{\mu\nu}\partial_\alpha f(\phi) &= \int d^4x\sqrt{-g}\left\{\Gamma^{\alpha}_{\mu\nu}\partial_\alpha f(\phi)+\frac{1}{2\sqrt{-g}}g_{\mu\nu}\partial_\rho\left[\sqrt{-g}g^{\alpha\rho}\right]\partial_\alpha f(\phi)\right. \\
&\quad \left.+\frac{1}{2}g_{\mu\nu}g^{\alpha\rho}\partial_\rho\partial_\alpha f(\phi)-\partial_\mu\partial_\nu f(\phi)\right\}\delta g^{\mu\nu} \\
&= \int d^4x\sqrt{-g}\left(-\frac{1}{2}T^2_{\mu\nu}\right)\delta g^{\mu\nu}, \qquad \text{(A.20)}
\end{aligned}
$$

where $T^2_{\mu\nu}$ is defined as

$$
\boxed{T^2_{\mu\nu}\equiv 2\partial_\mu\partial_\nu f(\phi)-2\Gamma^{\alpha}_{\mu\nu}\partial_\alpha f(\phi)-\tfrac{1}{\sqrt{-g}}g_{\mu\nu}\partial_\rho\left[\sqrt{-g}g^{\alpha\rho}\right]\partial_\alpha f(\phi)-g_{\mu\nu}g^{\alpha\rho}\partial_\rho\partial_\alpha f(\phi)}. \qquad \text{(A.21)}
$$

Finally, the first integral on the right-hand side of equation (A.4) becomes

$$
\int d^4x\sqrt{-g}\left[-\frac{1}{2}T^1_{\mu\nu}-\frac{1}{2}T^2_{\mu\nu}\right]\delta g^{\mu\nu}. \qquad \text{(A.22)}
$$

Using the relation $dg = gg^{\mu\nu}dg_{\mu\nu}$, the second integral on the right-hand side of equation (A.4) can be written as

$$
\begin{aligned}
\int d^4x f(\phi)R_{\mu\nu}\delta\left(\sqrt{-g}g^{\mu\nu}\right) &= \int d^4x\sqrt{-g}f(\phi)R_{\mu\nu}\delta g^{\mu\nu}+\int d^4x f(\phi)g^{\mu\nu}R_{\mu\nu}\delta\sqrt{-g} \\
&= \int d^4x\sqrt{-g}f(\phi)R_{\mu\nu}\delta g^{\mu\nu}-\int d^4x\frac{1}{2}\sqrt{-g}f(\phi)g^{\alpha\rho}R_{\alpha\rho}g_{\mu\nu}\delta g^{\mu\nu} \\
&= \int d^4x\sqrt{-g}\left\{f(\phi)R_{\mu\nu}-\frac{1}{2}g_{\mu\nu}f(\phi)R\right\}\delta g^{\mu\nu}, \text{ since } G_{\mu\nu}=R_{\mu\nu}-\tfrac{1}{2}g_{\mu\nu}R \\
&= \int d^4x\sqrt{-g}\left\{f(\phi)G_{\mu\nu}\right\}\delta g^{\mu\nu}. \qquad \text{(A.23}
\end{aligned}
$$

Since $\delta f(\phi)$ is zero, the third integral on the right-hand side of equation (A.4) vanishes. The variation of the second part of the integral (A.1) leads to the energy-momentum tensor of a scalar field, as follow:

First defining,

$$
\mathcal{L} \equiv \frac{1}{2}g^{\mu\nu}\partial_\mu\phi\partial_\nu\phi+V(\phi), \qquad \text{(A.24)}
$$

then it follows,

$$\delta\left(\sqrt{-g}\mathcal{L}\right) = \frac{\partial\left(\sqrt{-g}\mathcal{L}\right)}{\partial g^{\mu\nu}}\delta g^{\mu\nu} + \frac{\partial\left(\sqrt{-g}\mathcal{L}\right)}{\partial g^{\mu\nu}_{,\alpha}}\delta g^{\mu\nu}_{,\alpha}. \tag{A.25}$$

However, the second term of equation (A.25) can be rewritten as

$$\frac{\partial\left(\sqrt{-g}\mathcal{L}\right)}{\partial g^{\mu\nu}_{,\alpha}}\delta g^{\mu\nu}_{,\alpha} = \partial_\alpha\left\{\frac{\partial\left(\sqrt{-g}\mathcal{L}\right)}{\partial g^{\mu\nu}_{,\alpha}}\delta g^{\mu\nu}\right\} - \partial_\alpha\left(\frac{\partial\left(\sqrt{-g}\mathcal{L}\right)}{\partial g^{\mu\nu}_{,\alpha}}\right)\delta g^{\mu\nu}.$$

Therefore, equation (A.25) becomes

$$\delta\left(\sqrt{-g}\mathcal{L}\right) = \left[\frac{\partial\left(\sqrt{-g}\mathcal{L}\right)}{\partial g^{\mu\nu}} - \partial_\alpha\left(\frac{\partial\left(\sqrt{-g}\mathcal{L}\right)}{\partial g^{\mu\nu}_{,\alpha}}\right)\right]\delta g^{\mu\nu} + \partial_\alpha\left\{\frac{\partial\left(\sqrt{-g}\mathcal{L}\right)}{\partial g^{\mu\nu}_{,\alpha}}\delta g^{\mu\nu}\right\} \tag{A.26}$$

Using the above result, the second part of the integral (A.1) becomes

$$\begin{aligned}\delta\int d^4x\sqrt{-g}\mathcal{L} &= \int d^4x\left\{\frac{\partial\left(\sqrt{-g}\mathcal{L}\right)}{\partial g^{\mu\nu}} - \partial_\alpha\left(\frac{\partial\left(\sqrt{-g}\mathcal{L}\right)}{\partial g^{\mu\nu}_{,\alpha}}\right)\right\}\delta g^{\mu\nu} + (\text{vanishing surface term}) \\ &= \int d^4x\sqrt{-g}\left(\frac{1}{2}T^3_{\mu\nu}\right)\delta g^{\mu\nu},\end{aligned} \tag{A.27}$$

where $T^3_{\mu\nu}$ is defined as

$$T^3_{\mu\nu} \equiv \frac{2}{\sqrt{-g}}\left\{\frac{\partial\left(\sqrt{-g}\mathcal{L}\right)}{\partial g^{\mu\nu}} - \partial_\alpha\left(\frac{\partial\left(\sqrt{-g}\mathcal{L}\right)}{\partial g^{\mu\nu}_{,\alpha}}\right)\right\}. \tag{A.28}$$

Since $\mathcal{L}$ doesn't depend on $g^{\mu\nu}_{,\alpha}$, $T^3_{\mu\nu}$ becomes

$$\boxed{T^3_{\mu\nu} = \partial_\mu\phi\partial_\nu\phi - \tfrac{1}{2}g_{\mu\nu}\left(g^{\alpha\rho}\partial_\alpha\phi\partial_\rho\phi + 2V(\phi)\right)}. \tag{A.29}$$

Finally, using equations (A.22), (A.23) and (A.27), equation (A.3) becomes

$$\delta S = \int d^4x\sqrt{-g}\left\{f(\phi)G_{\mu\nu} - \frac{1}{2}T^1_{\mu\nu} - \frac{1}{2}T^2_{\mu\nu} - \frac{1}{2}T^3_{\mu\nu} - \frac{1}{2}T^B_{\mu\nu}\right\}\delta g^{\mu\nu} = 0, \tag{A.30}$$

where $T^B_{\mu\nu}$ is the energy-momentum tensor of background matter. Since equation (A.30) is valid for an arbitrary variation $\delta g^{\mu\nu}$, the integrand must be equal to zero.

Therefore,

$$G_{\mu\nu} = \frac{1}{2f(\phi)}\left[T^1_{\mu\nu} + T^2_{\mu\nu} + T^3_{\mu\nu} + T^B_{\mu\nu}\right]$$

$$\boxed{G_{\mu\nu} = \kappa T_{\mu\nu}}, \tag{A.31}$$

where $T_{\mu\nu}$, the *effective* energy-momentum tensor, is given by

$$\boxed{T_{\mu\nu} \equiv (1 - \xi\kappa\phi^2)^{-1}\left[T^1_{\mu\nu} + T^2_{\mu\nu} + T^3_{\mu\nu} + T^B_{\mu\nu}\right]}. \tag{A.32}$$

To illuminate the consequences of the coupling term, equations (A.31) could be rewritten as

$$G_{\mu\nu} = \kappa_{eff}\left[T^1_{\mu\nu} + T^2_{\mu\nu} + T^3_{\mu\nu} + T^B_{\mu\nu}\right], \tag{A.33}$$

where

$$\kappa_{eff} \equiv \frac{1}{2f(\phi)} = \kappa\left(1 - \xi\kappa\phi^2\right)^{-1}. \tag{A.34}$$

Therefore, the value of $\xi$ can be constrained by the measured time variation, or lack thereof, of the Newton's constant. Using solar–system measurements [5] have determined that $|\xi| \leq 10^{-2}$. My numerical calculations show that this coupling has insignificant consequences as long as the evolution of the universe is concerned.

# Appendix B

# Equation of Motion of the Scale Factor $R$

Herein is presented a full derivation of the equation of motion of the scale factor $R$.

The zero curvature $k = 0$ Robertson-Walker metric takes the form

$$ds^2 = -dt^2 + R^2(t)\left(dx^2 + dy^2 + dz^2\right). \tag{B.1}$$

For the metric (B.1), the only non-zero terms of the connection coefficient are:

$$\Gamma^1_{10} = \Gamma^2_{20} = \Gamma^3_{30} = \frac{1}{2}g^{11}g_{11,0} = H \equiv \frac{\dot{R}}{R} \tag{B.2}$$

$$\Gamma^0_{11} = \Gamma^0_{20} = \Gamma^0_{30} = -\frac{1}{2}g^{00}g_{11,0} = R\dot{R}, \tag{B.3}$$

and terms related by the symmetry $\Gamma^\alpha_{\mu\nu} = \Gamma^\alpha_{\nu\mu}$.

Therefore, the only non–zero terms of the Ricci tensor, which will be denoted $Ric$ from here on, are

$$Ric_{11} = Ric_{22} = Ric_{33} = \Gamma^0_{11,0} + \Gamma^0_{11}\Gamma^1_{10} = 2\dot{R}^2 + R\ddot{R} \tag{B.4}$$

$$Ric_{00} = -3\left[3\Gamma^0_{01,0} + \left(\Gamma^1_{10}\right)^2\right] = -3\left(\dot{H} + H^2\right). \tag{B.5}$$

Hence, the Ricci scalar curvature becomes,

$$Ric = g^{\mu\nu} Ric_{\mu\nu} = 3\left(\dot{H} + 3H^2 + \frac{\ddot{R}}{R}\right) = 6\left(\dot{H} + 2H^2\right), \tag{B.6}$$

where the last step follows directly from

$$\dot{H} = \partial_t\left(\frac{\dot{R}}{R}\right) = \frac{\ddot{R}}{R} - \left(\frac{\dot{R}}{R}\right)^2 = \frac{\ddot{R}}{R} - H^2. \tag{B.7}$$

Using these results, equation (A.31) gives

$$\begin{aligned} G_{00} &= Ric_{00} - \frac{1}{2} g_{00} Ric \\ &= -3\left(\dot{H} + H^2\right) + 3\left(\dot{H} + 2H^2\right) \\ &= 3H^2 = \kappa T_{00}, \text{ therefore} \\ H^2 &= \frac{\kappa}{3} T_{00}. \end{aligned} \tag{B.8}$$

Furthermore, the spatial components give

$$\begin{aligned} G_{11} = G_{22} = G_{33} &= Ric_{11} - \frac{1}{2} g_{11} Ric = 2\dot{R}^2 + R\dot{R} - 3R^2\left[\frac{\ddot{R}}{R} + \left(\frac{\dot{R}}{R}\right)^2\right] \\ &= -\dot{R}^2 - 2R\ddot{R} = \kappa T_{11}. \end{aligned} \tag{B.9}$$

Dividing equation (B.9) by $R^2$ and using equation (B.8)

$$\begin{aligned} \frac{\ddot{R}}{R} &= -\frac{1}{2}\left[R^{-2}\left(\kappa T_{11}\right) + \left(\frac{\dot{R}}{R}\right)^2\right] \\ &= -\frac{1}{2}\left[R^{-2}\left(\kappa T_{11}\right) + \frac{\kappa}{3} T_{00}\right] \\ &= -\frac{\kappa}{6}\left[T_{00} + 3R^{-2} T_{11}\right]. \end{aligned} \tag{B.10}$$

Putting equations (B.8) and (B.10) into equation (B.7) gives

$$\dot{H} = -\frac{\kappa}{6}\left[T_{00} + 3R^{-2} T_{11}\right] - \frac{\kappa}{3} T_{00}$$

$$= -\frac{\kappa}{2}\left[T_{00} + R^{-2}T_{11}\right]. \tag{B.11}$$

What is there left to do is to evaluate both $T_{00}$ and $T_{11}$. Before proceeding any further, it pays to investigate what restrictions are imposed on $T^B_{\mu\nu}$ by the assumption that the space–time is isotropic. In short, the energy-momentum tensor of the matter can be written in the form

$$T^{\mu\nu} = p_B g^{\mu\nu} + (\rho_B + p_B)\, u^\mu u^\nu, \tag{B.12}$$

where $u^\mu$ is a unit vector in the time direction and $\rho_B$ and $p_B$ are the energy density and pressure of matter, respectively.

Starting from $T^1_{00}$ (keeping in mind that $\sqrt{-g} = R^3$),

$$\begin{aligned}
T^1_{00} &= -\left\{R^{-3}\frac{\partial f(\phi)}{\partial t}\frac{\partial R^3}{\partial t} + \frac{\partial^2 f(\phi)}{\partial t^2}\right\} \\
&= -\left\{3H\frac{\partial f(\phi)}{\partial t} + \frac{\partial^2 f(\phi)}{\partial t^2}\right\}, && \text{(B.13)} \\
T^1_{00} &= \frac{\partial^2 f(\phi)}{\partial t^2} - R^{-3}\frac{\partial f(\phi)}{\partial t}\frac{\partial R^3}{\partial t} - \frac{\partial^2 f(\phi)}{\partial t^2} \\
&= \frac{\partial^2 f(\phi)}{\partial t^2} - 3H\frac{\partial f(\phi)}{\partial t}, && \text{(B.14)} \\
T^3_{00} &= \frac{1}{2}\dot{\phi}^2(t) + V(\phi), \text{ and} && \text{(B.15)} \\
T^B_{00} &= \rho_B. && \text{(B.16)}
\end{aligned}$$

Putting equations (B.13), (B.14), (B.15) and (B.16), and the following first and second time derivatives of $f(\phi)$,

$$\begin{aligned}
\frac{\partial f(\phi)}{\partial t} &= -\xi\phi\dot{\phi} && \text{(B.17)} \\
\frac{\partial^2 f(\phi)}{\partial t^2} &= -\xi\left(\dot{\phi}^2 + \phi\ddot{\phi}\right), && \text{(B.18)}
\end{aligned}$$

in equation (A.32), $T_{00}$ becomes,

$$\boxed{T_{00} = \left(1 - \xi\kappa\phi^2\right)^{-1}\left\{\rho_B + \tfrac{1}{2}\dot{\phi}^2 + V(\phi) + 6\xi H\phi\dot{\phi}\right\}}. \tag{B.19}$$

Similarly, starting from $T^1_{11}$,

$$\begin{aligned} T^1_{11} &= R^{-3}\frac{\partial f(\phi)}{\partial t}\frac{\partial R^3}{\partial t} + \frac{\partial^2 f(\phi)}{\partial t^2} \\ &= R^2\left(3H\frac{\partial f(\phi)}{\partial t} + \frac{\partial^2 f(\phi)}{\partial t^2}\right), \end{aligned} \tag{B.20}$$

$$\begin{aligned} T^2_{11} &= -2\Gamma^0_{11}\frac{\partial f(\phi)}{\partial t} + R^{-1}\frac{\partial f(\phi)}{\partial t} + R^2\frac{\partial^2 f(\phi)}{\partial t^2} \\ &= -2R\dot{R}\frac{\partial f(\phi)}{\partial t} + 3R\dot{R}\frac{\partial f(\phi)}{\partial t} + R^2\frac{\partial^2 f(\phi)}{\partial t^2} \\ &= R^2\left(H\frac{\partial f(\phi)}{\partial t} + \frac{\partial^2 f(\phi)}{\partial t^2}\right), \end{aligned} \tag{B.21}$$

$$T^3_{11} = R^2\left(\frac{1}{2}\dot{\phi}^2(t) - V(\phi)\right), \text{ and} \tag{B.22}$$

$$T^B_{11} = R^2 p_B. \tag{B.23}$$

Finally, using equations (B.17) and (B.18), (B.20), (B.21), (B.22) and (B.23), $T_{11}$ becomes,

$$T_{11} = \left(1-\xi\kappa\phi^2\right)^{-1} R^2\left\{p_B + \frac{1}{2}\dot{\phi}^2 - V(\phi) + 4H\frac{\partial f(\phi)}{\partial t} + 2\frac{\partial^2 f(\phi)}{\partial t^2}\right\}$$

$$\boxed{T_{11} = \left(1-\xi\kappa\phi^2\right)^{-1} R^2\left\{p_B + \tfrac{1}{2}\dot{\phi}^2 - V(\phi) - 4H\xi\phi\dot{\phi} - 2\xi\left(\dot{\phi}^2 + \phi\ddot{\phi}\right)\right\}}. \tag{B.24}$$

Finally, substituting equations (B.19) and (B.24) for $T_{00}$ and $T_{11}$, respectively, in equations (B.8) and (B.11), gives

$$\boxed{H^2 = \tfrac{\kappa}{3}\left(1-\xi\kappa\phi^2\right)^{-1}\left\{\rho_B + \tfrac{1}{2}\dot{\phi}^2 + V(\phi) + 6\xi H\phi\dot{\phi}\right\}}, \tag{B.25}$$

$$\boxed{\dot{H} = -\tfrac{\kappa}{2}\left(1-\xi\kappa\phi^2\right)^{-1}\left\{\rho_B + p_B + \dot{\phi}^2 + 2\xi\left(H\phi\dot{\phi} - \dot{\phi}^2 - \phi\ddot{\phi}\right)\right\}}. \tag{B.26}$$

# Appendix C

# Equation of Motion for $\phi$

Herein is presented the full derivation of the equation of motion of scalar fields, $\phi$, with a none–zero scalar field–curvature coupling term.

The only term of the action (A.1) that could depend on $\phi$ and $\partial_\alpha\phi$, after multiplying through by $-1$, are

$$S = \int d^4x\sqrt{-g}\left[\frac{1}{2}\xi\phi^2 R + \frac{1}{2}g^{\mu\nu}\partial_\mu\phi\partial_\nu\phi + V(\phi)\right]. \tag{C.1}$$

Setting the variation of the above action to zero,

$$\delta S = 0, \tag{C.2}$$

and defining

$$\mathcal{L} \equiv \frac{1}{2}\xi R\phi^2 + \frac{1}{2}g^{\mu\nu}\partial_\mu\phi\partial_\nu\phi + V(\phi), \tag{C.3}$$

it follows

$$\delta\left(\sqrt{-g}\mathcal{L}\right) = \frac{\partial\left(\sqrt{-g}\mathcal{L}\right)}{\partial\phi}\delta\phi + \frac{\partial\left(\sqrt{-g}\mathcal{L}\right)}{\partial\left(\partial_\alpha\phi\right)}\delta\left(\partial_\alpha\phi\right). \tag{C.4}$$

However, the second term of equation (C.4) can be rewritten as

$$\frac{\partial\left(\sqrt{-g}\mathcal{L}\right)}{\partial\left(\partial_\alpha\phi\right)}\delta\left(\partial_\alpha\phi\right) = \partial_\alpha\left\{\frac{\partial\left(\sqrt{-g}\mathcal{L}\right)}{\partial\left(\partial_\alpha\phi\right)}\delta\phi\right\} - \partial_\alpha\left(\frac{\partial\left(\sqrt{-g}\mathcal{L}\right)}{\partial\left(\partial_\alpha\phi\right)}\right)\delta\phi.$$

Therefore, equation (C.4) becomes

$$\delta\left(\sqrt{-g}\mathcal{L}\right) = \left[\frac{\partial\left(\sqrt{-g}\mathcal{L}\right)}{\partial\phi} - \partial_\alpha\left(\frac{\partial\left(\sqrt{-g}\mathcal{L}\right)}{\partial\left(\partial_\alpha\phi\right)}\right)\right]\delta\phi + \partial_\alpha\left\{\frac{\partial\left(\sqrt{-g}\mathcal{L}\right)}{\partial\left(\partial_\alpha\phi\right)}\delta\phi\right\}. \quad \text{(C.5)}$$

Using the above result, the variation of the action (C.1) becomes

$$\begin{aligned}\delta\int d^4x\sqrt{-g}\mathcal{L} &= \int d^4x\left\{\frac{\partial\left(\sqrt{-g}\mathcal{L}\right)}{\partial\phi} - \partial_\alpha\left(\frac{\partial\left(\sqrt{-g}\mathcal{L}\right)}{\partial\left(\partial_\alpha\phi\right)}\right)\right\}\delta\phi + \text{(vanishing surface term)} \\ &= \int d^4x\left\{\frac{\partial\left(\sqrt{-g}\mathcal{L}\right)}{\partial\phi} - \partial_\alpha\left(\frac{\partial\left(\sqrt{-g}\mathcal{L}\right)}{\partial\left(\partial_\alpha\phi\right)}\right)\right\}\delta\phi = 0. \quad \text{(C.6)}\end{aligned}$$

Since equation (C.6) is valid for an arbitrary variation $\delta\phi$, the integrand must be equal to zero. Therefore,

$$\frac{\partial\left(\sqrt{-g}\mathcal{L}\right)}{\partial\phi} - \partial_\alpha\left(\frac{\partial\left(\sqrt{-g}\mathcal{L}\right)}{\partial\left(\partial_\alpha\phi\right)}\right) = 0. \quad \text{(C.7)}$$

For the metric (B.1) and $\partial_i\phi = 0$, where $i = (1,2,3)$, equation (C.7) gives

$$\begin{aligned}R^3\left\{\frac{\partial\mathcal{L}}{\partial\phi}\right\} &= \partial_t R^3\frac{\partial\mathcal{L}}{\partial\left(\partial_\alpha\phi\right)} + R^3\partial_\alpha\left(\frac{\partial\mathcal{L}}{\partial\left(\partial_\alpha\phi\right)}\right) \\ R^3\left\{6\xi\left(\dot{H}+2H^2\right)\phi + V'(\phi)\right\} &= 3R^2\dot{R}\frac{\partial\mathcal{L}}{\partial\dot{\phi}} + R^3\partial_t\left(\frac{\partial\mathcal{L}}{\partial\dot{\phi}}\right) \\ R^3\left\{6\xi\left(\dot{H}+2H^2\right)\phi + V'(\phi)\right\} &= -3R^2\dot{R}\dot{\phi} - R^3\ddot{\phi}, \quad \text{(C.8)}\end{aligned}$$

where prime indicates the partial derivative with respect to $\phi$. Therefore,

$$\boxed{\ddot{\phi} + 3H\dot{\phi} + 6\xi\left(\dot{H}+2H^2\right)\phi + V'(\phi) = 0}. \quad \text{(C.9)}$$

The above derivations were presented for the sake of completeness. For reasons discussed in chapter 2, $\xi \approx 0$ is assumed in this thesis.

# Appendix D

# Java 2 SDK Packages

| Package Name | Description |
|---|---|
| java.util | Contains the collections framework, legacy collection classes, event model, date and time facilities, internationalization, and miscellaneous utility classes (a string tokenizer, a random-number generator, and a bit array) |
| java.util.zip | Provides classes for reading and writing the standard ZIP and GZIP file formats |
| java.text | Provides classes and interfaces for handling text, dates, numbers, and messages in a manner independent of natural languages |
| java.io | Provides for system input and output through data streams, serialization and the file system |
| java.math | Provides classes for performing arbitrary-precision integer arithmetic (BigInteger) and arbitrary-precision decimal arithmetic (BigDecimal) |
| java.awt | Contains all of the classes for creating user interfaces and for painting graphics and images |
| java.awt.event | Provides interfaces and classes for dealing with different types of events fired by AWT components |
| java.awt.geom | Provides the Java 2D classes for defining and performing operations on objects related to two-dimensional geometry |
| java.awt.print | Provides classes and interfaces for a general printing API |
| javax.swing | Provides a set of "lightweight" (all-Java language) components that, to the maximum degree possible, work the same on all platforms |
| javax.swing.border | Provides classes and interface for drawing specialized borders around a Swing component |
| javax.swing.event | Provides for events fired by Swing components |
| javax.swing.table | Provides classes and interfaces for dealing with javax.swing.JTable |
| javax.print | Provides the principal classes and interfaces for the JavaTM Print Service API |
| javax.print.attribute | Provides classes and interfaces that describe the types of JavaTM Print Service attributes and how they can be collected into attribute sets |
| javax.print.attribute.standard | Package javax.print.attribute.standard contains classes for specific printing attributes |

Table D.1: Primary Java 2 SDK Packages [10] employed in the development of QuintET.

# Bibliography


[1] A. Billyard and A. Coley. Interactions in scalar field cosmology. *Physical Review D*, 61(083503), March 2000.

[2] Sean M. Carroll. Quintessence and the Rest of the World. Aug 1998. astro–ph/9806099.

[3] Sean M. Carroll. The Cosmological Constant. Apr 2000. astro–ph/00004075.

[4] CERN. *http://root.cern.ch/root/.*

[5] Takeshi Chiba. Quintessence, the Gravitational Constant, and Gravity. Aug 1999. gr–qc/9903094.

[6] T. Matsumoto *et al. The Astrophysical Journal*, 329:567–571, 1988.

[7] S. Perlutter *et al.* [Supernova Cosmology Project Collaboration]. Measurement of $\Omega$ and $\Gamma$ from 42 High-Redshift Supernovae. Dec 1998. astro–ph/9812133.

[8] Alan. H. Guth. The Big Band and Cosmic Inflation. 1991 Oskar Klein Memorial Lecture, Center for Theoretical Physics, MIT, Sept 1992.

[9] Mathworks. *http://www.mathworks.com/.*

[10] Sun Microsystems. [JavaTM 2 Platform, Standard Edition, v 1.4.1 API Specification]. http://java.sun.com/j2se/1.4.1/docs/api/, 2002.

[11] John A. Peacock. *Cosmological Physics.* Cambridge University Press, 1999.

[12] F. Perrotta, C. Baccigalupi, and S. Materrese. Extended Quintessence. Sept 1999. astro–ph/9006066.

[13] A. Guth S. Blau and Harvard-Smithsonian Center for Astrophysics. Inflationary Cosmology. [Published in *300 Years of Gravitation*, eds: W. Hawking and W. Israel, Cambridge University Press, 1987], Oct 1986.

[14] P. Steinhardt, L. Wang, and I. Zlatev. Cosmological tracking solutions. *Physical Review D*, 59(123504), 1999.

[15] I. Zlatev, L. Wang, and P. Steinhardt. Quintessence, Cosmic Coincidence, and the Cosmological Constant. *Physical Review Letters*, 82(5):869–899, Feb 1999.